Article

Developmental Cell

KIF1A/UNC-104 Transports ATG-9 to Regulate Neurodevelopment and Autophagy at Synapses

Graphical Abstract

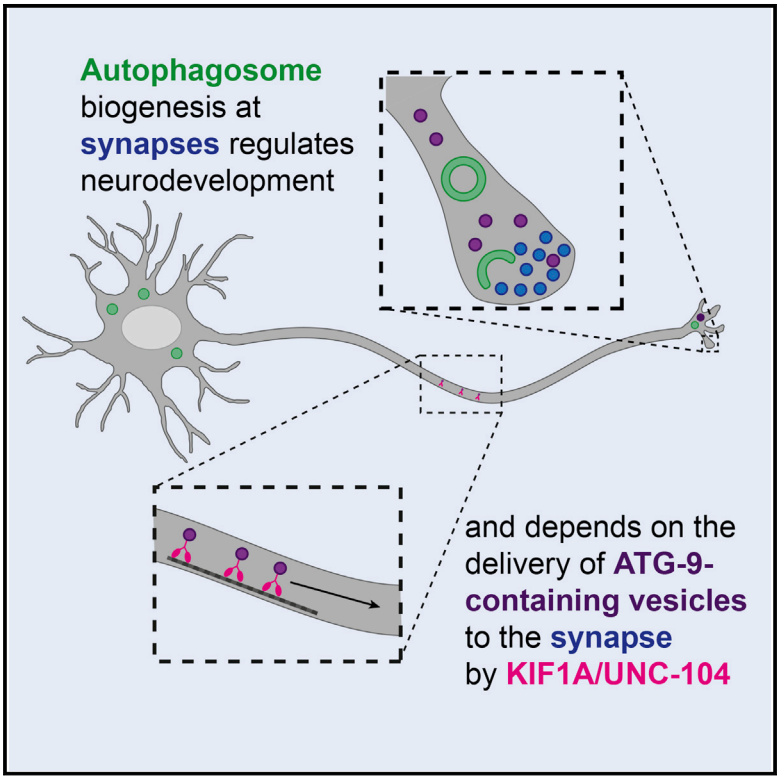

Authors

Andrea K.H. Stavoe, Sarah E. Hill, David H. Hall, Daniel A. Colón-Ramos

Correspondence

daniel.colon-ramos@yale.edu

In Brief

Autophagy is a degradation process important for neurodevelopment. Stavoe, Hill, et al. uncover spatial regulation of autophagy in *C. elegans* neurons. They show that autophagosomes form near synapses and are required for presynaptic assembly and axon outgrowth dynamics. Local autophagosome biogenesis depends on kinesin KIF1A/UNC-104-mediated transport of autophagy protein ATG-9.

Highlights

- The autophagy pathway is required for presynaptic assembly in vivo
- The autophagy pathway acts cell autonomously and in specific neurons in development
- Autophagosome biogenesis occurs in compartmentalized axonal regions near synapses
- The synaptic vesicle kinesin UNC-104/KIF1A transports ATG-9 to presynaptic sites

Stavoe et al., 2016, Developmental Cell *38*, 1–15
July 25, 2016
http://dx.doi.org/10.1016/j.devcel.2016.06.012

CellPress

Please cite this article in press as: Stavoe et al., KIF1A/UNC-104 Transports ATG-9 to Regulate Neurodevelopment and Autophagy at Synapses, Developmental Cell (2016), http://dx.doi.org/10.1016/j.devcel.2016.06.012

Developmental Cell
Article

KIF1A/UNC-104 Transports ATG-9 to Regulate Neurodevelopment and Autophagy at Synapses

Andrea K.H. Stavoe,[1,4] Sarah E. Hill,[1,4] David H. Hall,[2] and Daniel A. Colón-Ramos[1,3,*]
[1]Program in Cellular Neuroscience, Neurodegeneration and Repair, Departments of Cell Biology and Neuroscience, Yale University School of Medicine, 295 Congress Avenue, BCMM 436B, New Haven, CT 06536-0812, USA
[2]Center for *C. elegans* Anatomy, Albert Einstein College of Medicine, Bronx, NY 10461, USA
[3]Instituto de Neurobiología, Recinto de Ciencias Médicas, Universidad de Puerto Rico, 201 Boulevard del Valle, San Juan 00901, Puerto Rico
[4]Co-first author
*Correspondence: daniel.colon-ramos@yale.edu
http://dx.doi.org/10.1016/j.devcel.2016.06.012

SUMMARY

Autophagy is a cellular degradation process important for neuronal development and survival. Neurons are highly polarized cells in which autophagosome biogenesis is spatially compartmentalized. The mechanisms and physiological importance of this spatial compartmentalization of autophagy in the neuronal development of living animals are not well understood. Here we determine that, in *Caenorhabditis elegans* neurons, autophagosomes form near synapses and are required for neurodevelopment. We first determine, through unbiased genetic screens and systematic genetic analyses, that autophagy is required cell autonomously for presynaptic assembly and for axon outgrowth dynamics in specific neurons. We observe autophagosome biogenesis in the axon near synapses, and this localization depends on the synaptic vesicle kinesin, KIF1A/UNC-104. KIF1A/UNC-104 coordinates localized autophagosome formation by regulating the transport of the integral membrane autophagy protein, ATG-9. Our findings indicate that autophagy is spatially regulated in neurons through the transport of ATG-9 by KIF1A/UNC-104 to regulate neurodevelopment.

INTRODUCTION

Macroautophagy (hereafter called autophagy) is an evolutionarily conserved cellular degradation process best known for its role in cellular homeostasis (Feng et al., 2014; Marino et al., 2011; Son et al., 2012; Wu et al., 2013a; Zhang and Baehrecke, 2015). While autophagy is induced under stress conditions in yeast and many mammalian cells, in neurons, autophagosome formation is a constitutively active process (Lee, 2012; Wong and Holzbaur, 2015; Xilouri and Stefanis, 2010). Basal levels of autophagy are essential for neuronal survival, and neuron-specific inhibition of the autophagy pathway results in axonal degeneration and neuronal cell death (Hara et al., 2006; Komatsu et al., 2007; Yang et al., 2013; Yue et al., 2009).

Autophagy can regulate axon morphogenesis and synaptic physiology in neurons (Binotti et al., 2015; Hernandez et al., 2012; Rudolf et al., 2016; Shehata and Inokuchi, 2014; Torres and Sulzer, 2012; Yamamoto and Yue, 2014). For example, knockdown of the autophagic protein Atg7 in murine neurons results in longer axons, while activation of the autophagy pathway with rapamycin results in shorter neurites (Ban et al., 2013; Chen et al., 2013). In *Drosophila*, disruption of autophagy decreases the size of the neuromuscular junction, while induction of autophagy increases synaptic boutons and neuronal branches (Shen and Ganetzky, 2009). These changes in the axon are dependent, at least in part, on the degradation of cytoskeletal regulatory proteins and structures (Ban et al., 2013). Consistent with these observations, autophagosomes form at the tips of actively elongating axons in cultured neurons and contain membrane and cytoskeletal components (Bunge, 1973; Hollenbeck, 1993; Hollenbeck and Bray, 1987; Maday et al., 2012).

Most of our knowledge of autophagosome biogenesis comes from studies conducted either in yeast or mammalian cell culture (Abada and Elazar, 2014; Hale et al., 2013; Reggiori and Klionsky, 2013). Less is known about how autophagy is regulated in vivo in multicellular organisms during development and stress (Wu et al., 2013a; Zhang and Baehrecke, 2015). In developmental programs in metazoans, autophagy plays critical roles by degrading substrates at specific transitions (Hale et al., 2013; Tsukamoto et al., 2008; Wu et al., 2013a; Zhang et al., 2009). Autophagy also plays important roles during the development of the nervous system (Boland and Nixon, 2006; Cecconi et al., 2007; Lee et al., 2013; Yamamoto and Yue, 2014). However, the specific roles of autophagy in the coordination of neurodevelopmental events are less clear.

Neurons are highly polarized cells. In primary neurons, autophagosomes are observed to form at the distal end of the axon, indicating compartmentalization and spatial regulation of autophagosome biogenesis (Ariosa and Klionsky, 2015; Ashrafi et al., 2014; Hollenbeck, 1993; Hollenbeck and Bray, 1987; Maday and Holzbaur, 2014; Maday et al., 2012; Yue, 2007). Furthermore, autophagosome biogenesis requires the ordered recruitment of assembly factors to the distal axon (Maday and Holzbaur, 2014; Maday et al., 2012). How localized recruitment is regulated in neurons to specify autophagosome biogenesis is not well understood.

In this study, we conducted unbiased forward genetic screens to identify pathways involved in presynaptic assembly

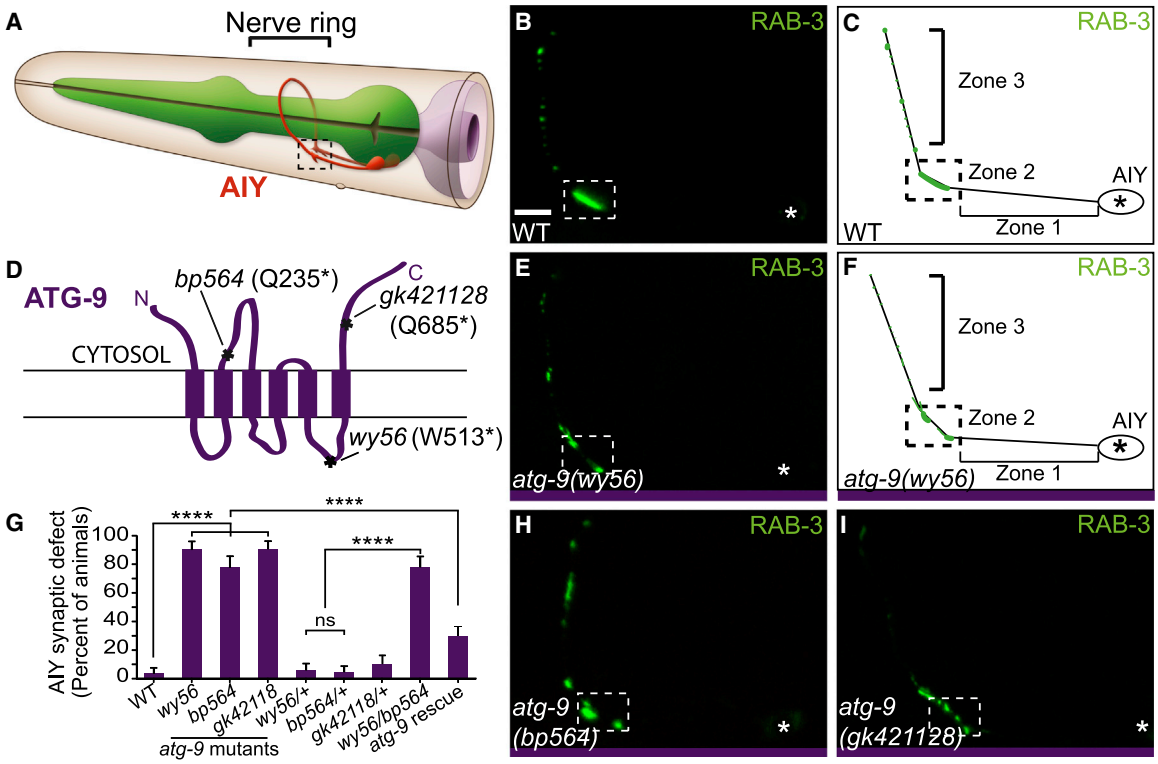

Figure 1. ATG-9 Is Required for AIY Synaptic Vesicle Clustering

(A) Schematic of AIY interneurons (red) in the nerve ring (indicated by bracket) in the head of the worm. Reprinted with permission from wormatlas.org (Z. Altun).

(B and C) Distribution of synaptic vesicles (visualized with GFP::RAB-3) in a representative wild-type animal (B) and represented in a schematic diagram (C). Throughout the text, zone 1 corresponds to an asynaptic region of the AIY neurite, zone 2 (enclosed by dashed box) corresponds to a synaptic-rich region in the dorsal turn of the neurite, and zone 3 corresponds to a synaptic region with intermittent presynaptic clusters. We focus the characterization of our phenotypes to zone 2, as described previously (Colón-Ramos et al., 2007; Stavoe et al., 2012; Stavoe and Colón-Ramos, 2012).

(D) Schematic of ATG-9 transmembrane domains with *bp564*, *wy56*, and *gk421128* lesions and corresponding protein effects indicated.

(E and F) Distribution of synaptic vesicles in an *atg-9(wy56)* mutant animal (E) and represented in a cartoon diagram (F).

(G) Quantification of the AIY presynaptic phenotype in wild-type, three *atg-9* mutant backgrounds, heterozygous *atg-9* animals, *atg-9 (wy56/bp564)* trans-heterozygotes, and *atg-9(bp464)* mutant animals that contain a pan-neuronal (*Punc-14*) *atg-9* rescuing construct. Error bars represent 95% confidence interval. ****$p < 0.0001$ between indicated groups by Fisher's exact test.

(H and I) Distribution of synaptic vesicles in *atg-9(bp564)* (H) and *atg-9(gk421128)* (I) mutant animals.

Each image is a maximal projection of a confocal z stack; the asterisk denotes the location of the cell body and the dashed box encloses AIY zone 2.

Scale bar in (B) for (B), (E), (H), and (I), 5 μm.

in *Caenorhabditis elegans* and identified an allele of *atg-9*. ATG-9 is known for its role in autophagosome biogenesis (Feng et al., 2016; Lang et al., 2000; Noda et al., 2000; Reggiori et al., 2004; Stanley et al., 2013; Wang et al., 2013; Yamamoto et al., 2012). Through genetic and cell biological approaches, we determined that the autophagy pathway is required cell autonomously to promote presynaptic assembly in the interneuron AIY. We performed systematic analyses with cell biological markers for cytoskeletal organization, active zone position, and synaptic vesicle clustering to establish that 18 distinct autophagy genes promote proper neurodevelopment in *C. elegans*. We examined different neuron types to determine that autophagy regulates synaptic positions and axon outgrowth in specific neurons. We found that ATG-9 is transported to the tip of growing neurites or to synaptic regions by the synaptic vesicle kinesin UNC-104/KIF1A. Transport of ATG-9, in turn, regulates synaptic autophagosome biogenesis. We propose that transport of ATG-9 by UNC-104/KIF1A confers spatial regulation of autophagy in neurons.

RESULTS

Mutant Allele *wy56* Displays Defects in AIY Synaptic Vesicle Clustering

During development, the AIY interneurons of *C. elegans* establish a stereotyped pattern of en passant (along the length of the axon) synaptic outputs. This pattern is reproducible across animals and displays specificity for both synaptic partners and positions (Figures 1A–1C and S1A) (Colón-Ramos et al., 2007; White et al., 1986). The positions of these en passant synapses in AIY are instructed by glia-derived Netrin, which directs local organization of the actin cytoskeleton, active zone localization, and synaptic vesicle clustering (Colón-Ramos et al., 2007; Stavoe et al., 2012; Stavoe and Colón-Ramos, 2012). To identify the mechanisms underlying these early events that organize synaptogenesis, we performed visual forward genetic screens using the synaptic vesicle marker GFP::RAB-3 in AIY. From these screens, we identified the allele *wy56*, which displays a highly

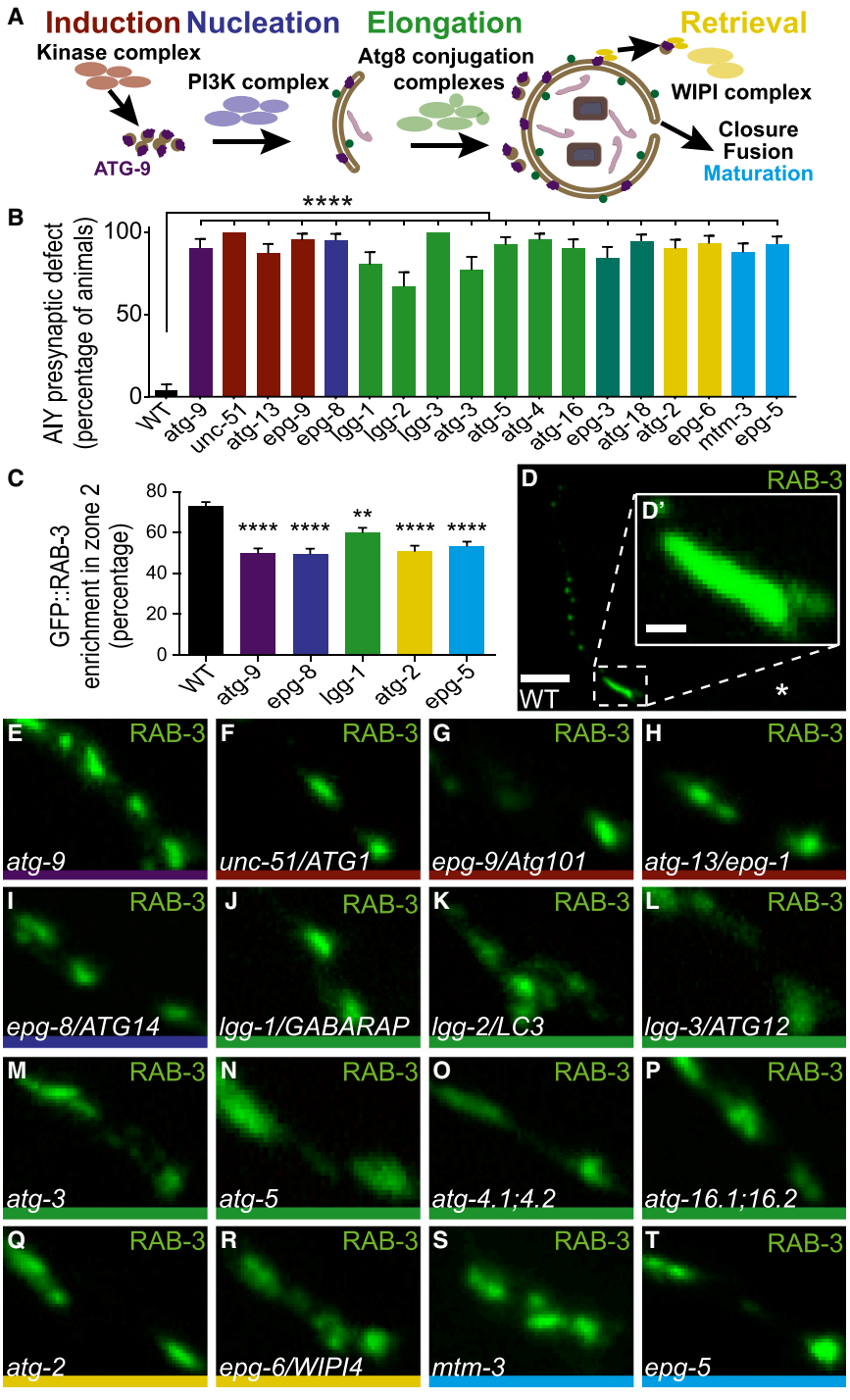

Figure 2. The Autophagy Pathway Is Required for AIY Synaptic Vesicle Clustering

(A) Schematic of the autophagosome biogenesis pathway, including the general stages: induction (red), nucleation (blue), elongation (green), retrieval (yellow), closure, fusion, and maturation (cyan).

(B) Quantification of the penetrance of the AIY presynaptic defect in wild-type and autophagy pathway mutant animals. For all genotypes quantified, n > 100 animals. Error bars represent 95% confidence interval. ****p < 0.0001 between autophagy mutants and wild-type by Fisher's exact test.

(C) Quantification of the relative distribution of GFP::RAB-3 in AIY zone 2 in wild-type and representative autophagy pathway mutants. For all genotypes quantified, n > 28 neurons. Error bars represent SEM. **p < 0.01, ****p < 0.0001 between autophagy mutants and wild-type by one-way ANOVA with Tukey's post hoc analysis.

(D) Distribution of synaptic vesicles (visualized with GFP::RAB-3) in a representative wild-type animal. (D′) Inset in (D) is enlarged zone 2 region from (D).

(E–T) Distribution of synaptic vesicles (visualized with GFP::RAB-3) in AIY zone 2 of *atg-9(gk421128)* (E), *unc-51(e369)* (F), *epg-9(bp320)* (G), *atg-13(bp414)* (H), *epg-8(bp251)* (I), *lgg-1(bp500)* (J), *lgg-2(tm5755)* (K), *lgg-3(tm1642)* (L), *atg-3(bp412)* (M), *atg-5(bp484)* (N), *atg-4.1(gk127286);atg-4.2(gk430078)* double mutants (O), *atg-16.1(gk668615);atg-16.2(gk145022)* double mutants (P), *atg-2(bp576)* (Q), *epg-6(bp242)* (R), *mtm-3(tm4475)* (S), and *epg-5(tm3425)* (T) mutant animals. Each image is a maximal projection of a confocal z stack; the asterisk denotes the location of the cell body and the dashed box encloses AIY zone 2 in (D). Only the AIY zone 2 region is depicted in (E)–(T), similar to the region depicted in (D′).

Scale bar in (D), 5 μm; scale bar in (D′) for (D′)–(T), 1 μm. See also Figures S1 and S2 and Table S1.

penetrant, abnormal distribution of synaptic vesicle proteins GFP::RAB-3 and SNB-1::YFP in the dorsal turn region of the AIY neurite (termed zone 2; enclosed in dashed box; Figures 1E–1G, 2B, 2C, and S1B).

We observed that both the penetrance and expressivity of *wy56* mutant animals resembled those of other synaptogenic mutants in AIY, including mutants of actin-organizing molecules CED-5/DOCK-180, CED-10/RAC-1, and MIG-10/Lamellipodin (Stavoe et al., 2012; Stavoe and Colón-Ramos, 2012). Also similar to these actin-organizing mutants, the *wy56* defective presynaptic pattern was observed early in development, at larval stage 1 (L1), just after hatching, suggesting that the phenotype emerges during embryogenesis (Figures S1I–S1O). Our findings indicate that *wy56* corresponds to a lesion in a gene required early in development for correct formation of presynaptic sites in AIY.

wy56 Is an Allele of Autophagy Gene *atg-9*

To identify the genetic lesion of *wy56*, we performed SNP mapping, whole-genome sequencing, and genetic rescue experiments. Our SNP mapping data indicate that *wy56* is located between 0.05 Mb and 0.5 Mb on chromosome V. Whole-genome

sequencing of *wy56* mutants revealed a point mutation in exon 8 of the *atg-9* (AuTophaGy-9) gene, resulting in a G to A nucleotide transition that converts W513 to an opal/umber stop codon (Figure 1D). Two independent alleles of *atg-9*, *atg-9(bp564)* and *atg-9(gk421128)*, with amber nonsense mutations at Q235 and Q685, respectively (Figure 1D) (Thompson et al., 2013; Tian et al., 2010), phenocopied the AIY presynaptic defect observed for *wy56* mutants (Figures 1G–1I). Consistent with *wy56* being an allele of *atg-9,* we also observed that *wy56* fails to complement *atg-9(bp564)* and that expression of the ATG-9 cDNA under an early panneuronal promoter (*punc-14*) rescues the *atg-9* presynaptic phenotype in AIY (Figure 1G). Together, our genetic data indicate that *wy56* is a nonsense, loss-of-function mutation in the *atg-9* gene.

The Autophagy Pathway Is Required for Synaptic Vesicle Clustering in AIY

The *atg-9* gene encodes a conserved, six-pass transmembrane protein that acts in the autophagy pathway (Lang et al., 2000; Noda et al., 2000; Young et al., 2006). Since ATG-9 is primarily known for regulating autophagosome biogenesis, we examined whether other components of the autophagy pathway are also required for synaptic vesicle clustering during synaptogenesis. Autophagosome biogenesis can be divided into four steps: initiation, nucleation, elongation, and retrieval. After biogenesis, autophagosomes mature prior to degradation of cargo. Distinct and specialized protein complexes mediate these steps, and homologs for these protein complexes have been identified in *C. elegans* (Figures 2A and S2I and Table S1) (Melendez and Levine, 2009; Tian et al., 2010). To evaluate the requirement of each of these distinct steps in synaptic vesicle clustering, we systematically examined existing alleles for each of these homologs using synaptic vesicle markers GFP::RAB-3 and SNB-1::YFP (Figures 2, S1, and S2, and Table S1).

Autophagy is induced by a kinase complex composed of UNC-51/Atg1/ULK, EPG-9/Atg101, and ATG-13/EPG-1 (Feng et al., 2014; Kamada et al., 2000; Melendez and Levine, 2009; Reggiori et al., 2004). Examination of putative null alleles for *unc-51/ATG1/ULK*, *epg-9/Atg101*, and *atg-13/epg-1* revealed highly penetrant AIY synaptic vesicle clustering defects that phenocopied those seen for *atg-9* mutant animals, as visualized with synaptic vesicle-associated markers GFP::RAB-3 and SNB-1::YFP (>87% penetrance; n > 100 animals for each genotype; Figures 2B, 2F–2H, and S1C, and Table S1), suggesting that the initiation complex of autophagy is required for synaptic vesicle clustering in AIY.

Nucleation is mediated by a PI3K complex that promotes fusion of ATG-9-containing vesicles into a phagophore (Kihara et al., 2001; Obara et al., 2006). The nucleation complex consists of LET-512/Vps34, BEC-1/Atg6, EPG-8/Atg14, and VPS-15 (Melendez and Levine, 2009). Most of these genes also play important roles in other essential cellular pathways, and for this reason, null mutations in these genes are unviable (Kihara et al., 2001; Obara et al., 2006; Yang and Zhang, 2011). However, we were able to examine a putative null allele for the nucleation gene *epg-8/ATG14*, which is specific to the autophagy pathway (Table S1) (Yang and Zhang, 2011). *epg-8* mutant animals exhibited highly penetrant AIY synaptic vesicle clustering defects as visualized with synaptic vesicle markers GFP::RAB-3 and SNB-1::YFP (95.4% of *epg-8* mutant animals, n = 108; Figures 2B, 2C, 2I, and S1D).

Once nucleated, the isolation membrane elongates via two ubiquitin-like conjugation complexes. In *C. elegans*, these complexes include LGG-1/GABARAP and LGG-2/LC3 (the two *C. elegans* Atg8 homologs) (Alberti et al., 2010; Manil-Segalen et al., 2014; Wu et al., 2015), LGG-3/Atg12, ATG-5, ATG-7, ATG-10, ATG-4 (ATG-4.1 and ATG-4.2 in *C. elegans*), ATG-16 (ATG-16.1 and ATG-16.2 in *C. elegans*), and ATG-3 (Melendez and Levine, 2009). EPG-3/VMP1 and ATG-18/WIP1/2 are also implicated in downstream stages of elongation (Lu et al., 2011; Tian et al., 2010). We examined putative null alleles for *atg-5, lgg-3/ATG12, lgg-1/GABARAP*, *lgg-2/LC3*, *epg-3*, *atg-18*, and a hypomorphic allele of *atg-3* (Table S1). Because *atg-4* and *atg-16* both have two homologs with redundant functions in *C. elegans* (Wu et al., 2012; Zhang et al., 2013), we built double mutant strains carrying putative null alleles for both homologs (*atg-4.1;atg-4.2* double mutants and *atg-16.1;atg-16.2* double mutants; Table S1). Consistent with elongation playing an important role in synaptic vesicle clustering in AIY, we observed that all elongation mutants display synaptic vesicle clustering defects in AIY that phenocopy the expressivity of other autophagy mutants (Figures 2B, 2C, 2J–2P, S1E, S1F, S2G, and S2H, and Table S1). We note that alleles of the *ATG8* homologs, *lgg-1* and *lgg-2*, display 80.7% and 67.3% penetrance, respectively. Since the *lgg-2(tm5755)* and *lgg-1(bp500)* alleles are putative nulls (Alberti et al., 2010; Manil-Segalen et al., 2014), our findings are consistent with these genes acting partially redundantly with each other or other autophagy machinery (Sato and Sato, 2011). *atg-3* mutants with hypomorphic allele *bp412* display 77.4% penetrance. The remaining elongation mutants, which are purported null alleles, display >85% penetrance (n > 100 animals for all genotypes quantified; Figures 2B, 2C, 2J–2P, S1E, S1F, S2G, and S2H, and Table S1).

Next, ATG-9 is recovered from the isolation membrane by a retrieval complex, the double membrane closes, and the autophagosome matures into an autolysosome (Cullup et al., 2013; Lu et al., 2011; Reggiori et al., 2004; Tian et al., 2010; Wang et al., 2001; Wu et al., 2014; Zhao et al., 2013). We observed that putative null alleles for retrieval genes *epg-6* and *atg-2* and maturation genes *mtm-3* and *epg-5* (Table S1) display defects in AIY synaptic vesicle clustering, as visualized by synaptic vesicle markers GFP::RAB-3 and SNB-1::YFP (>88% penetrance; n > 100 animals for all genotypes quantified; Figures 2B, 2C, 2Q–2T, S1G, and S1H).

Together, our findings indicate that components from all stages of the autophagy pathway are required for clustering of synaptic vesicle proteins in AIY during development. Our data further suggest that ATG-9 is acting within the autophagy pathway, not independently, to direct AIY synaptic vesicle clustering during development.

Selective Autophagy Genes *atg-11*, *epg-2*, and *sqst-1* Are Not Required for AIY Synaptic Vesicle Clustering

Autophagy is best known for its nonselective role in degrading bulk cytoplasm (Mizushima and Klionsky, 2007). In neurons, nonselective autophagy locally degrades membrane and cytoskeletal components at the tips of actively elongating axons (Ban et al., 2013; Chen et al., 2013; Hollenbeck and Bray,

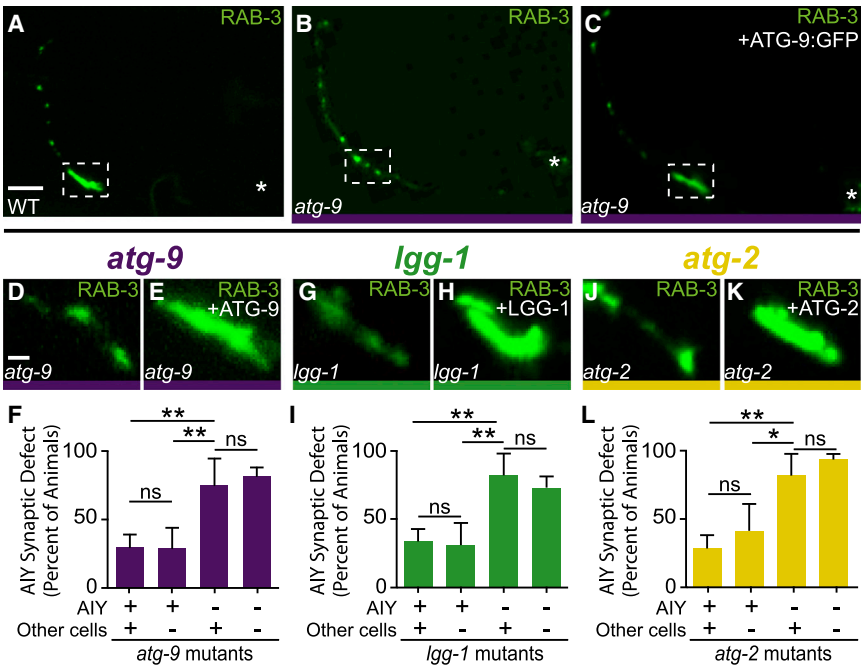

Figure 3. The Autophagy Pathway Acts Cell Autonomously to Instruct AIY Presynaptic Assembly

(A) Distribution of synaptic vesicles (visualized with GFP::RAB-3) in a representative wild-type animal.

(B and C) Distribution of synaptic vesicles (visualized with mCh::RAB-3, pseudocolored green) in an *atg-9(bp564)* mutant animal (B) and an *atg-9(bp564)* mutant expressing a panneuronal ATG-9::GFP rescuing construct (C).

(D–L) Distribution of synaptic vesicles in AIY zone 2 in *atg-9(bp564)* (D), *lgg-1(bp500)* (G), *atg-2(bp576)* (J) mutant animals and mutant animals expressing a corresponding rescuing array (E, H, and K). (F, I, and L) Quantification of rescue of autophagy mutant animals expressing unstable rescuing transgenes. Error bars represent 95% confidence interval. $^{**}p < 0.01$, $^{*}p < 0.05$ between indicated groups by Fisher's exact test.

Each image is a maximal projection of a confocal z stack; in (A)–(C), the asterisk denotes the location of the cell body and the dashed box encloses AIY zone 2. Scale bar in (A) for (A)–(C), 5 μm; scale bar in (D) for (D), (E), (G), (H), (J), and (K), 1 μm. See also Figure S3.

1987). However, the autophagy pathway can also selectively degrade specific organelles or target proteins in certain contexts. This process, known as selective autophagy, is dependent on the adaptor molecule Atg11, which interacts with cargo receptors to link specific protein targets to the autophagosome precursor membrane (Farre et al., 2013; He et al., 2006; Mao et al., 2013; Yorimitsu and Klionsky, 2005; Zaffagnini and Martens, 2016). Additional selective autophagy adaptors include the nematode-specific EPG-2 (Tian et al., 2010) and the *C. elegans* homolog of p62, SQST-1 (Table S1) (Lamark et al., 2009; Lin et al., 2013). To determine whether selective autophagy acts in AIY synaptic vesicle clustering, we examined putative null alleles for *atg-11*, *epg-2*, and *sqst-1* (Table S1). Unlike the other autophagy pathway mutants examined, we did not observe AIY presynaptic defects in these mutants (Figures S2B–S2D and data not shown). Therefore, our data suggest that selective autophagy adaptors ATG-11, EPG-2, and SQST-1 are not required for AIY synaptic vesicle clustering.

The Autophagy Pathway Acts Cell Autonomously in AIY to Promote Synaptic Vesicle Clustering

Next we examined whether autophagy acts cell autonomously in AIY by performing mosaic analyses with representative mutants from distinct steps of the autophagy pathway. Briefly, mitotically unstable rescuing arrays were used for each of the examined genes, and animals were scored for retention of the rescuing array in AIY and for the synaptic phenotype (Yochem and Herman, 2003). We observed that for *atg-9(bp564), lgg-1(bp500)* (elongation), and *atg-2(bp576)* (retrieval) mutants, retention of their rescuing arrays in AIY resulted in rescue of the AIY presynaptic defect, while retention of the array in other neurons (including postsynaptic partner RIA), but not in AIY, did not result in rescue of the AIY presynaptic defect (Figures 3D–3L). We also examined the endogenous expression pattern of *atg-9* and *atg-2* and observed that they are expressed in neurons, including AIY (Figures S3A–S3F). Together, our data suggest that the autophagy pathway acts cell autonomously in AIY to promote synaptic vesicle clustering.

The Autophagy Pathway Is Required for F-Actin Accumulation and Active Zone Protein Localization at Presynaptic Sites

To understand how autophagy regulates synaptic vesicle clustering in AIY, we examined the requirement of autophagy for the different elements of presynaptic assembly. In previous studies, we determined that AIY presynaptic sites are specified through the local organization of the actin cytoskeleton and active zone proteins (Colón-Ramos et al., 2007; Stavoe et al., 2012; Stavoe and Colón-Ramos, 2012). Therefore, we first examined whether active zone proteins and the actin cytoskeleton were correctly organized at presynaptic sites in autophagy mutants.

We observed that active zone protein SYD-1 is enriched and colocalizes with RAB-3 in AIY presynaptic regions in wild-type animals (Figures 4A–4C); however, in autophagy mutants, RAB-3 and SYD-1 are no longer enriched in the AIY zone 2 presynaptic region (Figures 4D–4I and S3G–S3R). Furthermore, we observed that autophagy mutants also affected the presynaptic enrichment of the F-actin probe UtrCH::GFP (Figures 4J–4O). Together, our data indicate that defects in autophagy affect the localization of F-actin, synaptic vesicles, and active zone proteins to presynaptic sites, and our data suggest that the autophagy pathway acts cell autonomously in AIY to promote synaptogenesis.

In AIY, synaptogenesis is regulated by glia-derived Netrin signaling. Netrin is required for the local clustering of its receptor, UNC-40/DCC, in AIY presynaptic regions. UNC-40/DCC then activates a signal transduction pathway in AIY, which includes

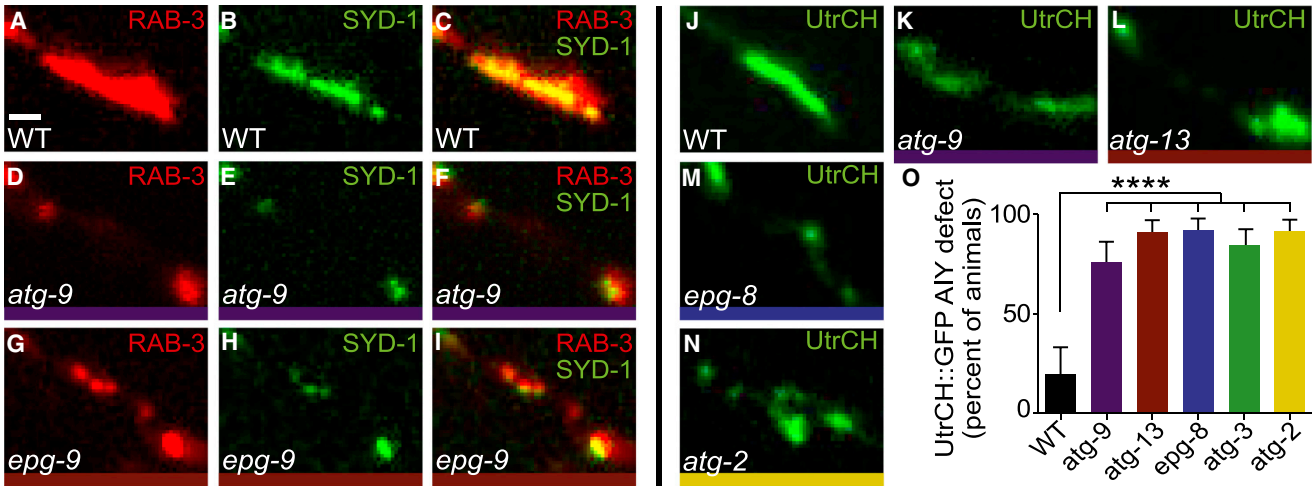

Figure 4. The Autophagy Pathway Is Required for Active Zone Assembly and F-Actin Organization

(A–I) Distribution of synaptic vesicles in AIY zone 2 (visualized with mCh::RAB-3), and localization of active zones in AIY (visualized with GFP::SYD-1) in wild-type (A–C), *atg-9(bp564)* (D–F), and *epg-9(bp320)* (G–I) mutant animals.

(J–N) F-actin organization in AIY zone 2 (visualized with UtrCH::GFP) in wild-type (J), *atg-9(bp564)* (K), *atg-13(bp414)* (L), *epg-8(bp251)* (M), and *atg-2(bp576)* (N) mutant animals.

(O) Quantification of penetrance of F-actin zone 2 enrichment defect in AIY. For all genotypes quantified, n > 50 animals. Error bars represent 95% confidence interval. ****$p < 0.0001$ between mutants and wild-type by Fisher's exact test.

Each image is a maximal projection of a confocal z stack; only AIY zone 2 is depicted. Scale bar in (A) for (A)–(N), 1 μm. See also Figure S4.

Rac GEF CED-5/DOCK180, MIG-10B/Lamellipodin, and ABI-1/Abl Interactor 1. This pathway culminates in the local organization of F-actin and synaptic vesicle clustering at presynaptic sites (Colón-Ramos et al., 2007; Stavoe et al., 2012; Stavoe and Colón-Ramos, 2012). To examine if autophagy regulates these early signaling events, we visualized glia morphology and the subcellular localization of UNC-40::GFP and MIG-10B::GFP in AIY. We were unable to detect any defects in the development or morphology of the glia that specifies presynaptic assembly in AIY (Figures S4A–S4F). Furthermore, visualization of the areas of contact between the glia and AIY by GFP reconstitution across synaptic partners (GRASP) (Feinberg et al., 2008; Shao et al., 2013) did not reveal defects in the AIY-glia contacts in any of the examined autophagy mutants (data not shown). We also did not detect defects in the subcellular localization of UNC-40 or MIG-10B in the examined autophagy mutants (Figures S4G–S4J). Our findings indicate that autophagy is not required for the development of the glia that specifies the synaptic positions in AIY or for the subcellular localization of UNC-40 and MIG-10B during synaptogenesis. Our data are consistent with autophagy acting in parallel to known synaptogenic signaling pathways to regulate synapse formation in AIY. Importantly, our findings indicate that autophagy is required in vivo and during development for actin organization, active zone assembly, and synaptic vesicle clustering.

Autophagosome Biogenesis Occurs at AIY Presynaptic Sites

In primary neuron culture, autophagosome biogenesis is spatially compartmentalized (Ariosa and Klionsky, 2015; Ashrafi et al., 2014; Bunge, 1973; Maday and Holzbaur, 2014; Maday et al., 2012; Yue, 2007). To determine when and where autophagosomes form in *C. elegans* neurons during development, we surveyed high-magnification transmission electron micrographs of neuronal somas and neurites in embryos. We observed autophagic vacuole (AV)-like organelles (identified by ultrastructural criteria as described (Bunge, 1973; Hernandez et al., 2012; Melendez et al., 2003; Yu et al., 2004; see also Experimental Procedures) in the cell bodies and neurites of developing embryonic neurons (Figures 5A–5C). Our findings are consistent with electron microscopy studies in primary neuron culture that reported the presence of autophagosomes in elongating axons (Bunge, 1973) and indicated that autophagosomes form in developing neurons in *C. elegans* embryos when axon outgrowth and synaptogenesis occur.

To understand the in vivo dynamics of autophagosomes in neurons, we examined the localization of autophagosomes in AIY using GFP::LGG-1. LGG-1 is the *C. elegans* homolog of Atg8/GABARAP, a molecule that is post-translationally modified to associate with autophagosomal membranes upon autophagy induction (Alberti et al., 2010; Kabeya et al., 2000; Kirisako et al., 1999; Lang et al., 1998; Mizushima et al., 2010; Tian et al., 2010; Zhang et al., 2015). Due to its dynamic but stable association with autophagosomes, GFP::LGG-1 and homologous markers are used as reliable cell biological probes for autophagosome dynamics (Manil-Segalen et al., 2014; Melendez et al., 2003; Mizushima et al., 2010; Tian et al., 2010; Zhang et al., 2015).

We observed that GFP::LGG-1 was diffusely cytoplasmic throughout the AIY neuron and localized to small puncta in the AIY cell body. In 38.5% of wild-type 3-fold embryos (n = 26), we also observed LGG-1 puncta in the AIY neurite located in the synapse-rich region (zone 2) (Figures 5D–5E). The localization pattern was similar post-embryonically in wild-type animals (n = 123) (Figures 5G and 5M). In addition, this subcellular localization was not observed when we expressed GFP::LGG-1(G116A) (Figures 5F, 5H, and 5M), which contains a point

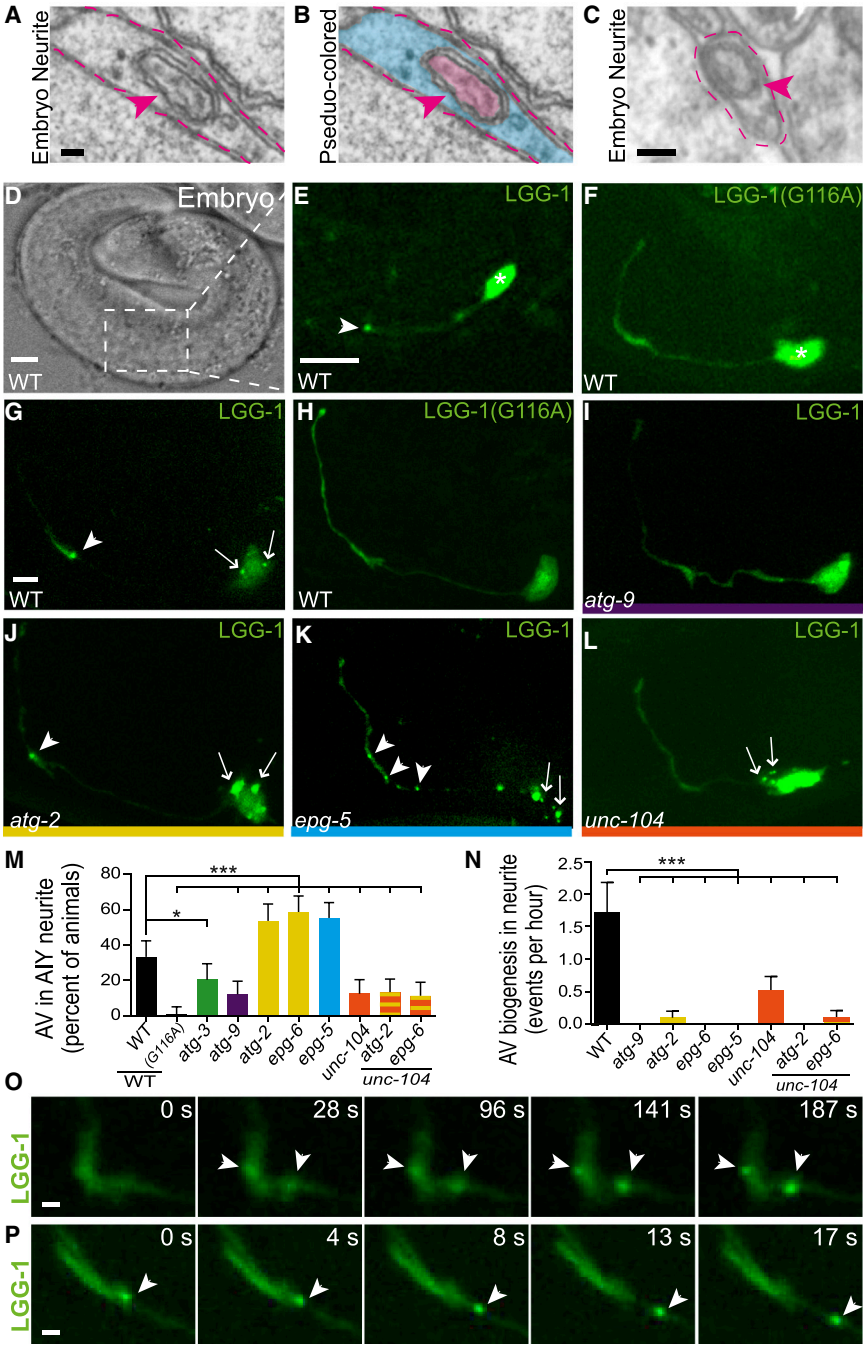

Figure 5. Autophagosome Biogenesis Occurs at AIY Presynaptic Sites during Development

(A–C) Transmission electron micrographs of autophagic vacuole (AV)-like organelles in embryonic neuronal processes of *C. elegans* during the developmental time of axon outgrowth and synaptogenesis. Images were originally acquired by Richard Durbin (Durbin, 1987) and represent 500-min-old embryo PR5_(PVPR) (A and B) and 550-min-old embryo RDE (C). In all images, dashed lines outline a cross-section of neurite; arrowheads indicate autophagosomes in neurite. Neurite and AV-like organelle in (A) is pseudocolored blue (neurite) and pink (AV) in (B).

(D) Transmitted light image of a *C. elegans* embryo for reference.

(E and F) Embryonic expression of GFP::LGG-1 (E) and GFP::LGG-1(G116A) (F) in AIY in a wild-type animal. LGG-1(G116A) is a point mutant incapable of associating with autophagosomes (Mizushima et al., 2010; Zhang et al., 2015). The asterisk denotes the location of the AIY cell body.

(G–L) Distribution of autophagosomes visualized with GFP::LGG-1 (G and I–L) or GFP::LGG-1(G116A) (H) in AIY in wild-type (G and H), *atg-9(bp564)* (I), *atg-2(bp576)* (J), *epg-5(tm3425)* (K), and *unc-104(e1265)* (L) mutant animals.

(M) Quantification of the penetrance of animals with LGG-1 puncta in the neurite of AIY in wild-type and mutant backgrounds. For all categories quantified, n > 100 animals. Error bars represent 95% confidence interval. *p < 0.05, ***p < 0.001 between mutants and wild-type by Fisher's exact test.

(N) Quantification of autophagosome (AV) biogenesis in the AIY neurite (as described in Experimental Procedures) in wild-type and mutant backgrounds (n > 10 videos per genotype). Error bars represent SEM. ***p < 0.001 between mutants and wild-type by one-way ANOVA with Tukey's post hoc analysis.

(O and P) Time series depicting autophagosome biogenesis (O) (see also Movie S1) and autophagosome retrograde movement (P) (see also Movie S4). In (E)–(L), (O), and (P), arrowheads denote the location of LGG-1 puncta in the neurite and arrows denote the location of LGG-1 puncta in the cell body. Each image is a maximal projection of a confocal z stack. Scale bars in (A) for (A) and (B), and in (C), 200 nm; in (D), in (E) for (E) and (F), in (G) for (G)–(L), 5 μm; in (O), in (P), 1 μm.

See also Figure S5 and Movies S1, S2, S3, and S4.

mutation that prevents LGG-1 lipidation and conjugation to autophagosomes (Mizushima et al., 2010; Zhang et al., 2015).

Next we examined GFP::LGG-1 in autophagy mutant backgrounds. LGG-1 fails to become conjugated to the autophagosome membrane in *atg-3* mutants (Ichimura et al., 2000; Tanida et al., 2002; Tian et al., 2010). We observed fewer GFP::LGG-1 puncta in *atg-3(bp412)* mutants in the AIY cell body and neurite, consistent with a reduction of LGG-1 association with autophagosomes in these hypomorphic mutants (n = 103; Figures 5M and S5B). We then examined GFP::LGG-1 in *atg-2(bp576)*, *epg-6(bp424)*, and *epg-5(tm3425)* mutants, all lesions in genes for late stages of autophagosome biogenesis and all known to result in the accumulation of defective autophagosomes (Figures 5J, 5K, 5M, and S5C) (Lu et al., 2011; Mizushima et al., 2010; Shintani et al., 2001; Tian et al., 2010; Zhang et al., 2015). As expected, we observed a higher penetrance of animals displaying puncta in AIY neurites (54% of *atg-2(bp576)* mutants, 59% of *epg-6(bp424)* mutants, and 55% of *epg-5(tm3425)* mutant animals; Figure 5M) when we blocked these late steps of the autophagy pathway. Together, our results indicate that

autophagosomes are present in the AIY cell body and near presynaptic sites.

To elucidate the in vivo dynamics of autophagosome biogenesis in AIY, we performed time-lapse imaging. In wild-type animals, we observed that a majority of the autophagosome biogenesis events in the neurite occurred in the synaptic regions, with 95% of them in the synaptic-rich zone 2, at an average rate of 1.7 events/hr (n = 20 events in 22 neurons; Figures 5N and 5O; Movies S1, S2, and S3). As expected, autophagosome biogenesis was reduced in autophagy mutants, with less than 0.1 events/hr observed for *atg-9*, *atg-2*, *epg-6*, and *epg-5* mutant animals (Figure 5N). Autophagosome biogenesis was also reduced for late autophagy mutants (*atg-2*, *epg-6*, *epg-5*), in which partial or stalled autophagosomes accumulate, suggesting a negative feedback loop in which a block in autophagosome maturation halts new biogenesis in vivo. In wild-type animals, the LGG-1 puncta that formed near presynaptic sites underwent retrograde trafficking, with 82% of motile autophagosomes (n = 50) trafficking toward the cell body (Figures 5P and S5F; Movie S4), an observation that is consistent with autophagosome trafficking studies in cultured mammalian neurons (Maday and Holzbaur, 2014; Maday et al., 2012).

Together, our results indicate that autophagosomes form in AIY near presynaptic sites and that autophagy is required for synaptogenesis. The observed spatial compartmentalization for autophagosome biogenesis in *C. elegans* neurons is consistent with findings from cultured vertebrate neurons, in which autophagosomes were observed to locally form in growth cones of actively elongating axons (Bunge, 1973; Hollenbeck, 1993; Hollenbeck and Bray, 1987; Maday et al., 2012). We extend those observations to show that local autophagosome biogenesis in neurons also occurs in vivo, near synapses, and during development. Therefore, local autophagosome biogenesis in neurons is conserved, and compartmentalized autophagosome biogenesis may be important for function.

ATG-9 Localizes to AIY Presynaptic Regions in an UNC-104/KIF1A-Dependent Manner

Local autophagy has been hypothesized to be critical for degrading substrates in axonal subcellular structures (Hollenbeck, 1993; Hollenbeck and Bray, 1987). How local autophagy is regulated to confer spatial selectivity during substrate degradation is not well understood. To determine how the location of autophagy is specified, we examined the subcellular localization of ATG-9, the only multipass transmembrane protein that is part of the core autophagy pathway (Feng et al., 2014; Noda et al., 2000; Young et al., 2006). In the nerve ring, we observed that the subcellular localization of a rescuing ATG-9::GFP transgene was reminiscent of that of a panneuronally expressed synaptic vesicle-associated protein, RAB-3 (Figures 6A, 6D, and 6E) (Mahoney et al., 2006). We then examined the endogenous localization of ATG-9 by creating transgenic animals in which the genomic *atg-9* locus was modified with a CRISPR-based knockin of ATG-9::GFP (Figure 6B). C-terminal addition of GFP to ATG-9 does not disrupt its function (Figures 3A–3C and data not shown). Consistent with ATG-9 localizing to synaptic sites, we observed that the endogenous localization of ATG-9 was similar to panneuronally expressed GFP::RAB-3 and ATG-9::GFP in both adults and 3-fold embryos (Figures 6C–6G and 6I–6J). To better understand the subcellular localization of ATG-9, we expressed ATG-9::GFP cell specifically in AIY. Consistent with the endogenous expression pattern, we observed that ATG-9 was enriched in presynaptic regions and colocalized with RAB-3 in AIY (Figures 6L–6N). Our findings indicate that ATG-9 localizes to presynaptic sites in neurons.

ATG-9 is required for autophagosome biogenesis (Feng et al., 2016; He et al., 2009; Lang et al., 2000; Orsi et al., 2012; Reggiori and Tooze, 2012; Wang et al., 2013; Yamamoto et al., 2012; Young et al., 2006). In yeast, Atg9 localizes to small vesicles that nucleate to form the phagophore (Suzuki et al., 2015; Wang et al., 2013; Yamamoto et al., 2012). To understand how ATG-9 localizes to synaptic regions, we examined its subcellular localization in mutants for kinesins implicated in neuronal transport. UNC-14, a kinesin-1/KIF5 adaptor for neuronal transport of vesicles and synaptic precursors, interacts with UNC-51/ATG-1 to regulate axon outgrowth and neurodevelopment (Abe et al., 2009; Brown et al., 2009; Lai and Garriga, 2004; Ogura et al., 1997; Sakamoto et al., 2005). We did not observe any defects in synaptic vesicle clustering or ATG-9 localization in *unc-14(e57)* mutants (data not shown). Similarly, *unc-116(e2310)* mutants lacking the kinesin-1/KIF5 heavy chain and *unc-16(ju146)* mutants lacking kinesin-1/KIF5 regulator JIP3/Sunday Driver also did not display defects in ATG-9 localization (data not shown) (Byrd et al., 2001; Patel et al., 1993; Sakamoto et al., 2005; Yang et al., 2005).

However, examination of the synaptic vesicle kinesin UNC-104/KIF1A revealed a requirement for this kinesin in ATG-9 transport. In *unc-104(e1265)* mutant animals, synaptic vesicles fail to be transported to synapses and are instead restricted to the cell body (Hall and Hedgecock, 1991; Otsuka et al., 1991). Interestingly, we observed that in *unc-104(e1265)* mutant animals, ATG-9 does not localize to the nerve ring in embryos and adults (Figures 6H and 6K). Similarly, ATG-9 does not localize to AIY synaptic regions, and its localization is restricted to the cell body (Figures 6O–6Q). Our findings indicate that ATG-9 localizes to presynaptic sites in an UNC-104/KIF1A-dependent manner.

Autophagosome Biogenesis in Synaptic Regions Is Dependent on UNC-104/KIF1A

UNC-104/KIF1A is a neuron-specific motor protein that regulates anterograde axonal transport of synaptic vesicle precursors (Otsuka et al., 1991). UNC-104/KIF1A-regulated distribution of synaptic vesicles and active zone proteins controls the spatial distribution of synapses during development (Wu et al., 2013b). Therefore, by regulating the transport of synaptic cargo to precise sites during development, the kinesin-3 UNC-104/KIF1A provides spatial specificity for synaptogenesis.

Given the observed role of UNC-104/KIF1A in transporting ATG-9 to presynaptic sites and the known role of ATG-9 in autophagosome biogenesis, we hypothesized that localization of ATG-9 by UNC-104/KIF1A would regulate the spatial distribution of autophagosomes to presynaptic sites. To test this hypothesis, we first observed autophagosomes in *atg-9* mutant animals. Consistent with our hypothesis, in *atg-9* mutant animals, we detected significant reductions in the number of animals with autophagosomes in the AIY neurite (12% of *atg-9*

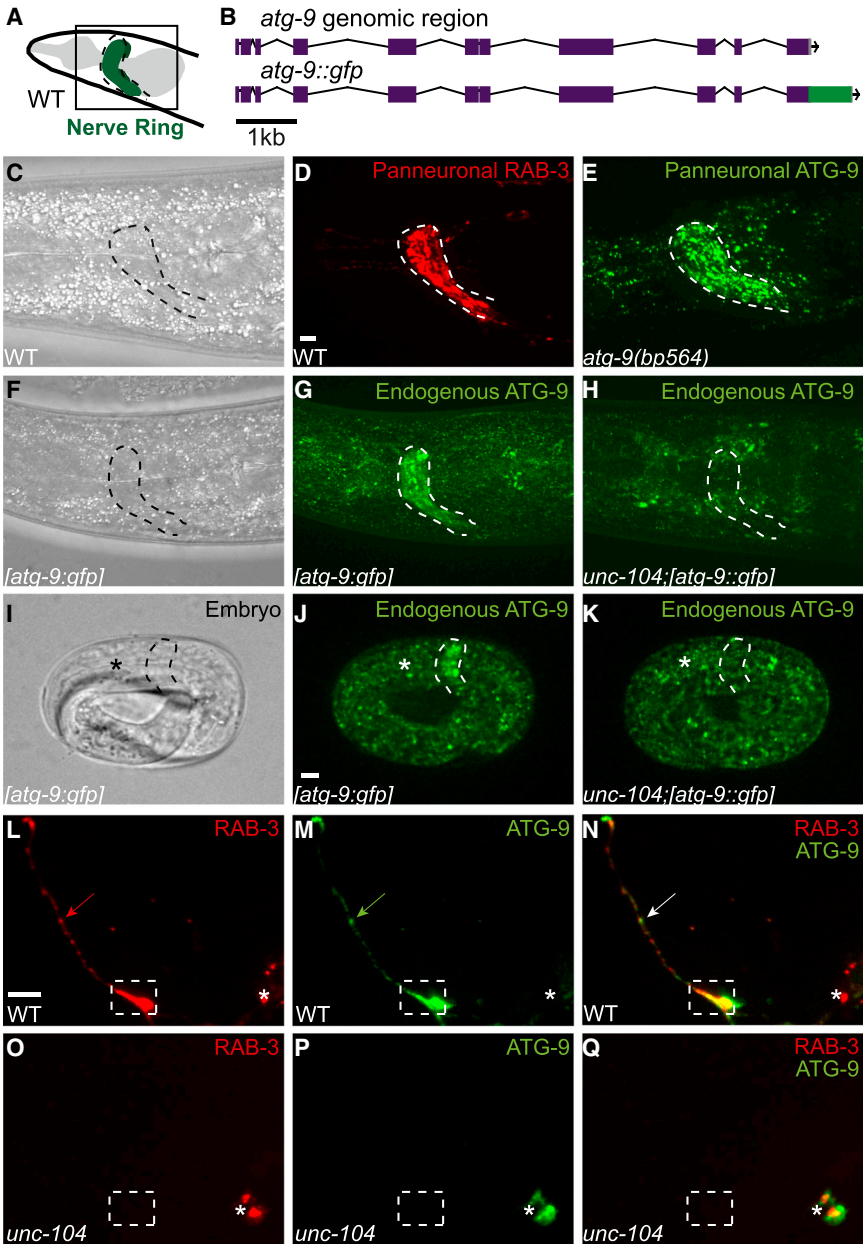

Figure 6. ATG-9 Transport to AIY Presynaptic Zones Requires KIF1A/UNC-104

(A) Schematic of the nematode nerve ring (green, encircled by a dotted line) in *C. elegans*.

(B) Schematic of the *atg-9* genomic region in a wild-type genome (top) and in the enhanced GFP CRISPR knockin (bottom).

(C and D) Location of the nerve ring, referenced with a transmitted light image (C) and visualized with GFP::RAB-3 (pseudocolored red) expressed panneuronally with *Prab-3* in a wild-type animal (D).

(E) Visualization of the subcellular localization of panneuronal ATG-9 (ATG-9::GFP rescuing array expressed with *Punc-14*).

(F–K) Distribution of endogenous ATG-9 as visualized by CRISPR insertion of enhanced GFP at the C terminus of the genomic *atg-9* (schematized in (B)) in adult (F–H) and embryo (I–K) in wild-type (G and J) and *unc-104(e1265)* mutant (H and K) animals. Anterior end of the embryo (head) is indicated with an asterisk in (I)–(K).

(L–Q) Distribution of synaptic vesicles (visualized with mCh::RAB-3) (L and O) and ATG-9::GFP (M and P) in AIY (merge in N and Q) in wild-type (L–N) and *unc-104(e1265)* mutant animals (O–Q). In (L)–(Q), the asterisk denotes the location of the AIY cell body; the dashed box encloses AIY zone 2.

Each image is a maximal projection of a confocal z stack. Scale bar in (D) for (C)–(H), in (J) for (I)–(K), and in (L) for (L)–(Q), 5 μm.

mutant animals, compared with 33% of wild-type animals) and in the rate of autophagosome biogenesis in the neurite (we did not observe any biogenesis events in *atg-9* mutants, n = 20 neurons, compared with 1.7 events/hr in wild-type, n = 22 neurons) (Figures 5I, 5M, and 5N). We next examined the requirement of UNC-104/KIF1A for autophagosome enrichment in synaptic regions by visualizing GFP::LGG-1 in *unc-104(e1265)* mutants. While autophagosomes are still present in AIY cell bodies in *unc-104(e1265)* hypomorphic mutant animals (Figure 5L), we observed significant reductions in the number of animals with GFP::LGG-1 puncta in the AIY neurite (13% of *unc-104* mutant animals; Figure 5M) and the rate of autophagosome biogenesis in the neurite (0.5 events/hr) (Figure 5N).

If UNC-104/KIF1A is important for local formation of autophagosomes, then it should act upstream of late autophagy genes *atg-2* and *epg-6* to suppress the accumulation of autophagosomes seen in these mutants. Indeed, we observed that *atg-2(bp576);unc-104(e1265)* and *epg-6(bp424);unc-104(e1265)* double mutants exhibited a significant reduction in the accumulation of autophagosomes in AIY presynaptic regions compared with *atg-2(bp576)* and *epg-6(bp424)* single mutants, indicating that *unc-104* is epistatic to *epg-6* and *atg-2* (Figures 5M, S5D, and S5E). Together our findings indicate that the presence of autophagosomes in synaptic regions is dependent on UNC-104/KIF1A and suggest that UNC-104/KIF1A regulates the spatial distribution of autophagosomes to presynaptic sites by mediating transport of ATG-9.

Autophagy Is Required in PVD for Axon Outgrowth

To better understand the role of autophagy in neurodevelopment, we examined multiple neuron classes in autophagy mutants for defects in neurodevelopmental events, including axon outgrowth, axon guidance, and synaptic positioning. Interestingly, most of the neurons examined (HSN, RIA, DA9, RIB, and NSM) did not display phenotypes in the examined categories (Figures S6A–S6F and data not shown). In the nociceptive sensory neuron PVD (Figure 7A), we observed that autophagy was required for the length of the PVD axon at larval stage 4

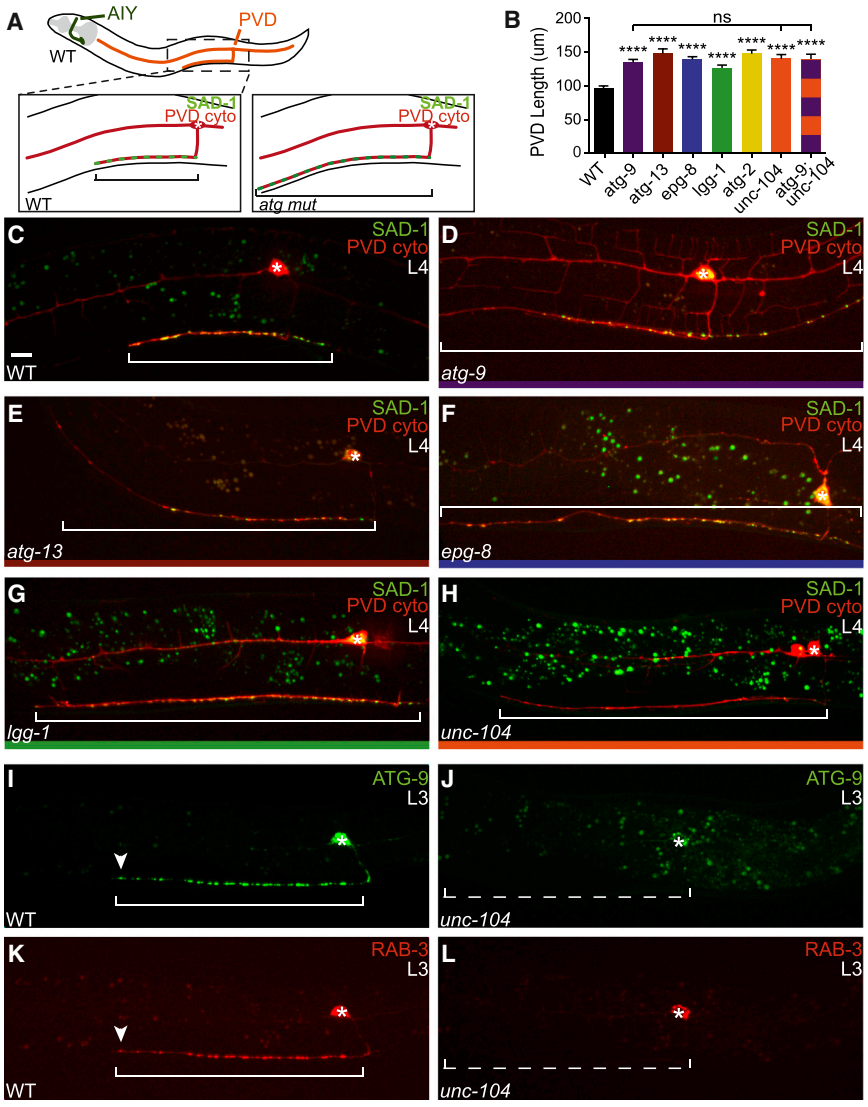

Figure 7. The Autophagy Pathway Regulates the Rate of PVD Axon Outgrowth

(A) Diagram of AIY (dark green) and PVD (orange) neurons in *C. elegans*. Schematics of PVD axon morphology (red) and presynaptic sites (light green) in wild-type (left box) and autophagy mutant animals (right box).

(B) Quantification of PVD axon length in wild-type and mutant L4 animals. Error bars represent SEM. ****$p < 0.0001$ between mutants and wild-type by one-way ANOVA with Tukey's post hoc analysis.

(C–H) PVD morphology (visualized with cytoplasmic mCh) and presynapses (visualized with SAD-1::GFP) in the axon of PVD in wild-type (C), *atg-9(bp564)* (D), *atg-13(bp414)* (E), *epg-8(bp251)* (F), *lgg-1(bp500)* (G), and *unc-104(e1265)* (H) mutant L4 animals.

(I–L) Distribution of ATG-9::GFP (I and J) and synaptic vesicles (visualized with mCh::RAB-3) (K and L) in PVD in wild-type (I and K) and *unc-104(e1265)* mutant animals (J and L). Arrowheads denote the tip of the axon in wild-type animals (I and K).

Each image is a maximal projection of a confocal z stack; the asterisk denotes the location of the cell body; the bracket denotes length of the PVD axon; and the dotted bracket (J and L) denotes the PVD axon (not visible due to the absence of presynaptic protein localization). Scale bar in (C) for (C)–(L), 5 μm. See also Figure S6.

(L4), but not for the morphology or timing of dendritic branching (Figures 7A–7G and data not shown).

The PVD axon begins to grow during larval stage 2 (L2) and continues to grow along the ventral nerve cord into adulthood (Maniar et al., 2012; Smith et al., 2010). To understand the requirement of autophagy in PVD axon outgrowth, we measured PVD axon length in L3, L4, and adult stages in wild-type and autophagy pathway mutant animals. We observed that the rate of PVD axon outgrowth in autophagy mutants was significantly higher than the rate observed in wild-type animals; this phenotype could be rescued upon neuronal expression of wild-type copies of the respective autophagy genes, each representing a distinct step of autophagy (Figures 7B–7G, S6G, and S6H). These data demonstrate that autophagy is required to regulate the rate of PVD axon outgrowth during development and are consistent with previous studies that demonstrated that knockdown of autophagy proteins results in longer axons (Ban et al., 2013). Our findings also indicate that autophagy is required in individual neurons to regulate distinct and specific neurodevelopmental events in vivo.

UNC-104/KIF1A Is Required for ATG-9 Localization and Axon Outgrowth in PVD

We next examined the localization of ATG-9 in PVD. Similar to AIY, we observed that ATG-9::GFP localizes in a punctate pattern in the PVD axon (Figure 7I) and colocalizes with the synaptic vesicle marker mCh::RAB-3 (Figure 7K). Interestingly, we observed that in actively elongating neurons, both ATG-9::GFP and mCh::RAB-3 localize to the growing tip of the PVD axon (Figures 7I and 7K; arrowheads). In *unc-104(e1265)* mutant animals, both ATG-9 and RAB-3 did not localize to presynaptic sites or to the tip of the PVD axon and were observed instead in the PVD cell body (Figures 7J and 7L). These data suggest that, in PVD, as in AIY, UNC-104/KIF1A is important for the transport of ATG-9 in the axon.

In PVD, *atg-9* mutants, like other autophagy mutants, display longer axons than wild-type animals (Figures 7B and 7D). We hypothesized that if UNC-104/KIF1A was required in PVD for ATG-9 localization and autophagy, *unc-104* mutants would phenocopy *atg-9* mutant animals, with longer PVD axons. Consistent with our hypothesis, we observed that *unc-104(e1265)* mutants phenocopied the *atg-9* mutant PVD axon length phenotype (Figures 7B and 7H). To our knowledge, this is the first time an axon outgrowth phenotype has been noted for the synaptic vesicle kinesin UNC-104/KIF1A. We hypothesized that if this newfound phenotype emerged from defects in ATG-9 transport, then *unc-104(e1265);atg-9(bp564)* double mutants would not enhance the length

of either single mutant. Indeed, genetic analyses of *unc-104(e1265);atg-9(bp564)* double mutant animals revealed no enhancement of the PVD axon length of either single mutant, consistent with our model that *unc-104* and *atg-9* act in the same pathway to regulate PVD axon outgrowth (Figure 7B). Together our findings suggest that UNC-104/KIF1A is important for ATG-9 transport, which in turn regulates localized autophagy and neurodevelopmental events.

DISCUSSION

Autophagy regulates specific neurodevelopmental events in vivo. Less is known about the roles of autophagy in the execution of neurodevelopmental programs, especially in the context of intact, living animals. Our systematic, in vivo and single-cell analyses of the roles of autophagy during neurodevelopment indicate that autophagy is required for distinct and specific stages of neurodevelopment in different neuron types of *C. elegans*. We observe that in the interneuron AIY, autophagy is required to regulate presynaptic assembly, and 18 distinct autophagy mutants display consistent and specific defects in synaptogenesis. In a different neuron (sensory neuron PVD), autophagy is specifically required to regulate the rate of axon outgrowth. However, autophagy is not required for the neurodevelopment of all neurons. Therefore, in vivo, autophagy plays precise and cell-specific roles during development to contribute to the formation of the nervous system.

Our cell biological and genetic evidence suggest that autophagy controls neurodevelopment by directly or indirectly regulating cytoskeletal structures in the axon. During development, neuronal structures such as synapses and growth cones are dynamically formed, altered, or eliminated in response to developmental cues (Kolodkin and Tessier-Lavigne, 2011). Underlying the transitions during neurodevelopment are mechanisms that regulate cytoskeletal dynamics (Nelson et al., 2013; Shen and Cowan, 2010). In our study, we found that autophagy mutants phenocopied previously identified mutations in genes that regulate the cytoskeleton during presynaptic assembly (Colón-Ramos et al., 2007; Stavoe et al., 2012; Stavoe and Colón-Ramos, 2012). We also found that disruption of the autophagy pathway in AIY results in disordered cytoskeletal structures, abnormal active zones, and mislocalized synaptic vesicles. Our findings are consistent with studies in *Drosophila* that demonstrate that autophagy regulates the development of neuromuscular junctions and with studies in vertebrates that demonstrate that autophagy-dependent changes in axon length rely on the degradation of cytoskeletal regulatory proteins (Ban et al., 2013; Shen and Ganetzky, 2009). Furthermore, our data complement studies that establish that, in actively elongating axons, autophagosomes at the tip of axons contain cytoskeletal components (Hollenbeck and Bray, 1987) and studies that show that induction of autophagy results in degradation of cytoskeletal components and inhibition of neurite outgrowth (Chen et al., 2013). We note that loss of autophagy in neurons does not result in the pleiotropic defects one would expect from general loss of cytoskeletal regulation or cellular homeostasis. Instead, autophagy mutants display precise neurodevelopmental phenotypes in specific neurons, suggesting that regulation of autophagy is required during development. In yeast and mammalian cells, autophagosome size and number are tightly controlled through transcriptional and post-translational mechanisms (Jin and Klionsky, 2014a, 2014b). We hypothesize that similar mechanisms might regulate the precise deployment of autophagosomes in metazoan neurons, thereby modulating controlled degradation of cytoskeletal structures during neurodevelopmental transitions.

Our study demonstrates that autophagosome biogenesis is compartmentalized in the axons of living animals. Previous studies have demonstrated that autophagosome biogenesis occurs in the distal axons of cultured neurons, suggesting a regulated segregation of autophagosome biogenesis in neurons (Bunge, 1973; Hollenbeck, 1993; Hollenbeck and Bray, 1987; Maday and Holzbaur, 2014; Maday et al., 2012). We now show that compartmentalization of autophagosome biogenesis in neurons is also observed in vivo and that autophagosomes are enriched in synaptic regions in both adult and embryonic animals. This synaptic enrichment might confer a regulatory step by localizing the spatial activity of this cellular degradation pathway.

We find that local transport of ATG-9-containing vesicles acts as a permissive cue to compartmentalize autophagosome biogenesis. Most autophagy proteins are cytosolic, and their association with the autophagosome can be induced through post-translational modifications (Xie et al., 2015). However, ATG-9 is a six-pass transmembrane protein and the only integral membrane protein that is part of the core machinery of the autophagy pathway (Lang et al., 2000; Noda et al., 2000; Young et al., 2006). In yeast, Atg9 localizes to small (30–60 nm) vesicles and promotes the formation of the autophagosome precursor (or isolation) membrane (Yamamoto et al., 2012). Little is known regarding the regulated transport of these Atg9-containing vesicles or if their transport limits the sites of autophagosome biogenesis. In our study, we observed that ATG-9 localizes to presynaptic regions and to the tip of the growing axon. Our findings in *C. elegans* neurons are consistent with studies in mammalian neurons, which demonstrate that Atg9 is enriched in varicosities in axons and colocalizes with synaptic proteins (Tamura et al., 2010). We determined that the localization of ATG-9 to the axon is regulated by the synaptic vesicle kinesin UNC-104/KIF1A, likely through the transport of ATG-9-containing vesicles. Disruption of ATG-9 transport in *unc-104* mutants resulted in reduced rates of autophagosome biogenesis and a reduced number of animals with autophagosomes in AIY neurites. Our findings provide mechanistic insights on how transport of the integral membrane protein ATG-9 provides spatial specificity of autophagosome biogenesis to presynaptic compartments and the distal axon.

Taken together, we propose the following model to explain how local regulation of autophagy during development could both restrain axon outgrowth in PVD and promote presynaptic assembly in AIY. We hypothesize that the UNC-104/KIF1A-dependent delivery of ATG-9 to the PVD growth cone is required for autophagy to remodel the growth cone, potentially through degradation of growth cone components. This results in slower growth cone velocity, while loss of autophagy results in unrestricted axon outgrowth in PVD. This model is consistent with findings from cell culture and mammalian neurons, which reveal that disruption of autophagy results in longer neurites,

while promotion of autophagy results in shorter neurites (Ban et al., 2013; Chen et al., 2013). In AIY, formation of the synaptic-rich region zone 2 is partially instructed by the extracellular cue Netrin (Colón-Ramos et al., 2007). We hypothesize that, after AIY axon outgrowth, autophagy may be important for locally remodeling subcellular structures, such as the cytoskeleton, to facilitate presynaptic assembly in the synaptic-rich AIY zone 2. Thus, in both AIY and PVD, autophagy may be required during neurodevelopment to locally remove cytoskeletal structures remaining from axon outgrowth to facilitate the creation of new functional domains in the subsequent stages of neurodevelopment.

In summary, our findings suggest that in neurons of living animals, regulated transport of autophagy components, such as ATG-9, permits compartmentalized autophagosome biogenesis and progression of neurodevelopmental events. Autophagy has also been implicated in postdevelopmental events in neurons, such as synaptic transmission and vesicle recycling (Binotti et al., 2015; Hernandez et al., 2012; Wang et al., 2015). Although we focused on the characterization of developmental phenotypes, we note that autophagy protein expression persists in adults and hypothesize that the mechanisms reported here could influence synaptic physiology and function postdevelopmentally.

EXPERIMENTAL PROCEDURES

For extended Experimental Procedures, please see Supplemental Experimental Procedures.

CRISPR Transgenics

We used a CRISPR protocol (Dickinson et al., 2015) to create *atg-9(ola270[atg-9::gfp::SEC])*, in which the enhanced GFP coding sequence and the self-excision cassette are inserted in place of the *atg-9* stop codon, and *atg-9(ola274 [atg-9::gfp])*, in which the self-excision cassette is excised.

Electron Micrographs

We surveyed hundreds of high-magnification electron micrographs from the archives of the Center for *C. elegans* Anatomy (Hall lab) to look for evidence of autophagy in embryonic neurons. The archive includes images contributed by Richard Durbin, John White (MRC/LMB, Cambridge), and Carolyn Norris (Hedgecock lab), many of which are publically available on www.wormimage.org. Neuronal autophagic vacuole-like organelles were identified as previously described (Bunge, 1973; Hernandez et al., 2012; Melendez et al., 2003; Yu et al., 2004). Autophagosomes in *C. elegans* are relatively small, owing to the small size of nematode cells (Melendez et al., 2003). We include the provenance of selected micrographs in the figure legends.

AIY and PVD Quantifications

AIY Presynaptic Defect

To quantify the penetrance of the AIY presynaptic defect, we used the integrated transgenic line *wyIs45* in the specified mutant backgrounds and quantified penetrance as previously described (Colón-Ramos et al., 2007; Stavoe et al., 2012; Stavoe and Colón-Ramos, 2012). Briefly, zone 2 was defined morphologically as the region of the AIY process, which turns dorsally from the anterior ventral nerve cord into the nerve ring in adult animals. We scored the number of animals displaying normal or abnormal zone 2 synaptic patterns relative to wild-type animals.

GFP::RAB-3 *Enrichment in AIY*

To quantify the enrichment of GFP::RAB-3 in AIY zone 2, we measured the total fluorescence intensity across the AIY zone 2 and zone 3 regions in confocal maximal projection micrographs. Enrichment was defined as the total fluorescence intensity of zone 2 divided by the total fluorescence intensity of both zones 2 and 3. Fluorescence intensity (after background subtraction) was determined by tracing the AIY neurite using the line scan function in FIJI (Schindelin et al., 2012). For this quantification, zone 2 was defined as 20% of the length of the entire AIY synaptic region (zones 2 and 3).

GFP::LGG-1 *in AIY*

The GFP::LGG-1 probe used in these studies is the same one that has been validated in *C. elegans* by immuno-labeling electron microscopy studies with both anti-GFP and anti-LGG-1 and used to examine the in vivo dynamics of autophagosomes in hypodermal seam cells and early embryos (Manil-Segalen et al., 2014; Melendez et al., 2003; Tian et al., 2010; Zhang et al., 2015). To quantify the penetrance of autophagosome (GFP::LGG-1) puncta in the AIY neurite, we scored for the presence or absence of LGG-1 puncta in the AIY neurite. For the rates of autophagosome biogenesis, we captured confocal micrographs (z stacks) once every minute for 30 min. We counted the number of GFP::LGG-1 puncta that appeared within the movie and report these as biogenesis events in Figure 5N.

Statistical Analyses

We used Fisher's exact test to determine statistical significance for categorical data. Error bars represent 95% confidence intervals.

Statistical significance for continuous data was determined using one-way ANOVA with post hoc analysis by Tukey's multiple comparisons test or Student's t test using PRISM software. Error bars for continuous data were calculated using SEM.

SUPPLEMENTAL INFORMATION

Supplemental Information includes Supplemental Experimental Procedures, six figures, one table, and four movies and can be found with this article online at http://dx.doi.org/10.1016/j.devcel.2016.06.012.

AUTHOR CONTRIBUTIONS

A.K.H.S., S.E.H., and D.A.C.R. designed the experiments; A.K.H.S. and S.E.H. performed the experiments and data analyses. S.E.H., D.H.H., and D.A.C.R. examined the electron micrographs for autophagosomes. A.K.H.S., S.E.H., and D.A.C.R. prepared the manuscript.

ACKNOWLEDGMENTS

We thank members of the Colón-Ramos lab, Erika Holzbaur (University of Pennsylvania), Hannes Buelow (Albert Einstein College of Medicine), and Alicia Meléndez (Queens College, CUNY) for their thoughtful comments on the manuscript and the project. We are particularly indebted to Kang Shen (Stanford University) for reagents, thoughtful comments, and advice during the course of this project. We thank summer interns Jihane Jadi (University of North Carolina, Chapel Hill) and Ninoshka Caballero-Colón (University of Puerto Rico, Humacao) for experimental assistance. We thank the *Caenorhabditis* Genetics Center for mutant strains, Cori Bargmann (Rockefeller University) for CX9797 (*kyIs445*) strain, David Miller (Vanderbilt University) for NC1686 (*wdIs51*) strain, the Mitani laboratory of the Tokyo Women's Medical University School of Medicine for autophagy mutant strains, and the Hong Zhang laboratory at the Institute of Biophysics, Chinese Academy of Sciences for autophagy mutant alleles. We thank Z. Altun (www.wormatlas.org) for diagrams used in the figures. We thank Bob Goldstein (University of North Carolina at Chapel Hill) for CRISPR self-excision cassette (SEC) constructs and advice. We are grateful to Steven Cook for his help in choosing and copying high-resolution electron micrographs from the Hall lab archive. We thank John White and Jonathan Hodgkin for their help in contributing thousands of electron micrographs from the MRC/LMB collection to the Hall lab. We thank the Research Center for Minority Institutions program and the Instituto de Neurobiología de la Universidad de Puerto Rico for providing a meeting and brainstorming platform. This work was partially conducted at the Marine Biological Laboratories at Woods Hole, under a Whitman research award to D.A.C.R. This work was funded by NIH grants to D.A.C.R. (U01HD075602, R01NS076558, and R24OD016474). D.H.H., the Center of *C. elegans* Anatomy, and www.wormimage.org were supported by NIH OD 010943. A.K.H.S. and S.E.H. were supported by Cellular and Molecular Biology

Training grant T32-GM007223 from the NIH. S.E.H. was also supported by NSF Graduate Research Fellowship DGE-1122492.

Received: December 7, 2015
Revised: May 9, 2016
Accepted: June 9, 2016
Published: July 7, 2016

REFERENCES

Abada, A., and Elazar, Z. (2014). Getting ready for building: signaling and autophagosome biogenesis. EMBO Rep. *15*, 839–852.

Abe, N., Almenar-Queralt, A., Lillo, C., Shen, Z., Lozach, J., Briggs, S.P., Williams, D.S., Goldstein, L.S., and Cavalli, V. (2009). Sunday driver interacts with two distinct classes of axonal organelles. J. Biol. Chem. *284*, 34628–34639.

Alberti, A., Michelet, X., Djeddi, A., and Legouis, R. (2010). The autophagosomal protein LGG-2 acts synergistically with LGG-1 in dauer formation and longevity in *C. elegans*. Autophagy *6*, 622–633.

Ariosa, A.R., and Klionsky, D.J. (2015). Long-distance autophagy. Autophagy *11*, 193–194.

Ashrafi, G., Schlehe, J.S., LaVoie, M.J., and Schwarz, T.L. (2014). Mitophagy of damaged mitochondria occurs locally in distal neuronal axons and requires PINK1 and Parkin. J. Cell Biol. *206*, 655–670.

Ban, B.K., Jun, M.H., Ryu, H.H., Jang, D.J., Ahmad, S.T., and Lee, J.A. (2013). Autophagy negatively regulates early axon growth in cortical neurons. Mol. Cell. Biol. *33*, 3907–3919.

Binotti, B., Pavlos, N.J., Riedel, D., Wenzel, D., Vorbruggen, G., Schalk, A.M., Kuhnel, K., Boyken, J., Erck, C., Martens, H., et al. (2015). The GTPase Rab26 links synaptic vesicles to the autophagy pathway. Elife *4*, e05597.

Boland, B., and Nixon, R.A. (2006). Neuronal macroautophagy: from development to degeneration. Mol. Aspects Med. *27*, 503–519.

Brown, H.M., Van Epps, H.A., Goncharov, A., Grant, B.D., and Jin, Y. (2009). The JIP3 scaffold protein UNC-16 regulates RAB-5 dependent membrane trafficking at *C. elegans* synapses. Dev. Neurobiol. *69*, 174–190.

Bunge, M.B. (1973). Fine structure of nerve fibers and growth cones of isolated sympathetic neurons in culture. J. Cell Biol. *56*, 713–735.

Byrd, D.T., Kawasaki, M., Walcoff, M., Hisamoto, N., Matsumoto, K., and Jin, Y. (2001). UNC-16, a JNK-signaling scaffold protein, regulates vesicle transport in *C. elegans*. Neuron *32*, 787–800.

Cecconi, F., Di Bartolomeo, S., Nardacci, R., Fuoco, C., Corazzari, M., Giunta, L., Romagnoli, A., Stoykova, A., Chowdhury, K., Fimia, G.M., et al. (2007). A novel role for autophagy in neurodevelopment. Autophagy *3*, 506–508.

Chen, J.X., Sun, Y.J., Wang, P., Long, D.X., Li, W., Li, L., and Wu, Y.J. (2013). Induction of autophagy by TOCP in differentiated human neuroblastoma cells lead to degradation of cytoskeletal components and inhibition of neurite outgrowth. Toxicology *310*, 92–97.

Colón-Ramos, D.A., Margeta, M.A., and Shen, K. (2007). Glia promote local synaptogenesis through UNC-6 (netrin) signaling in *C. elegans*. Science *318*, 103–106.

Cullup, T., Kho, A.L., Dionisi-Vici, C., Brandmeier, B., Smith, F., Urry, Z., Simpson, M.A., Yau, S., Bertini, E., McClelland, V., et al. (2013). Recessive mutations in EPG5 cause Vici syndrome, a multisystem disorder with defective autophagy. Nat. Genet. *45*, 83–87.

Dickinson, D.J., Pani, A.M., Heppert, J.K., Higgins, C.D., and Goldstein, B. (2015). Streamlined genome engineering with a self-excising drug selection cassette. Genetics *200*, 1035–1049.

Durbin, R.M. (1987). Studies on the Development and Organization of the Nervous System of *Caenorhabditis elegans* (University of Cambridge). http://www.wormatlas.org.

Farre, J.C., Burkenroad, A., Burnett, S.F., and Subramani, S. (2013). Phosphorylation of mitophagy and pexophagy receptors coordinates their interaction with Atg8 and Atg11. EMBO Rep. *14*, 441–449.

Feinberg, E.H., Vanhoven, M.K., Bendesky, A., Wang, G., Fetter, R.D., Shen, K., and Bargmann, C.I. (2008). GFP Reconstitution across Synaptic Partners (GRASP) defines cell contacts and synapses in living nervous systems. Neuron *57*, 353–363.

Feng, Y., He, D., Yao, Z., and Klionsky, D.J. (2014). The machinery of macroautophagy. Cell Res. *24*, 24–41.

Feng, Y., Backues, S.K., Baba, M., Heo, J.M., Harper, J.W., and Klionsky, D.J. (2016). Phosphorylation of Atg9 regulates movement to the phagophore assembly site and the rate of autophagosome formation. Autophagy *12*, 648–658.

Hale, A.N., Ledbetter, D.J., Gawriluk, T.R., and Rucker, E.B., 3rd (2013). Autophagy: regulation and role in development. Autophagy *9*, 951–972.

Hall, D.H., and Hedgecock, E.M. (1991). Kinesin-related gene unc-104 is required for axonal transport of synaptic vesicles in C. elegans. Cell *65*, 837–847.

Hara, T., Nakamura, K., Matsui, M., Yamamoto, A., Nakahara, Y., Suzuki-Migishima, R., Yokoyama, M., Mishima, K., Saito, I., Okano, H., et al. (2006). Suppression of basal autophagy in neural cells causes neurodegenerative disease in mice. Nature *441*, 885–889.

He, C., Song, H., Yorimitsu, T., Monastyrska, I., Yen, W.L., Legakis, J.E., and Klionsky, D.J. (2006). Recruitment of Atg9 to the preautophagosomal structure by Atg11 is essential for selective autophagy in budding yeast. J. Cell Biol. *175*, 925–935.

He, C., Baba, M., and Klionsky, D.J. (2009). Double duty of Atg9 self-association in autophagosome biogenesis. Autophagy *5*, 385–387.

Hernandez, D., Torres, C.A., Setlik, W., Cebrian, C., Mosharov, E.V., Tang, G., Cheng, H.C., Kholodilov, N., Yarygina, O., Burke, R.E., et al. (2012). Regulation of presynaptic neurotransmission by macroautophagy. Neuron *74*, 277–284.

Hollenbeck, P.J. (1993). Products of endocytosis and autophagy are retrieved from axons by regulated retrograde organelle transport. J. Cell Biol. *121*, 305–315.

Hollenbeck, P.J., and Bray, D. (1987). Rapidly transported organelles containing membrane and cytoskeletal components: their relation to axonal growth. J. Cell Biol. *105*, 2827–2835.

Ichimura, Y., Kirisako, T., Takao, T., Satomi, Y., Shimonishi, Y., Ishihara, N., Mizushima, N., Tanida, I., Kominami, E., Ohsumi, M., et al. (2000). A ubiquitin-like system mediates protein lipidation. Nature *408*, 488–492.

Jin, M., and Klionsky, D.J. (2014a). Regulation of autophagy: modulation of the size and number of autophagosomes. FEBS Lett. *588*, 2457–2463.

Jin, M., and Klionsky, D.J. (2014b). Transcriptional regulation of ATG9 by the Pho23-Rpd3 complex modulates the frequency of autophagosome formation. Autophagy *10*, 1681–1682.

Kabeya, Y., Mizushima, N., Ueno, T., Yamamoto, A., Kirisako, T., Noda, T., Kominami, E., Ohsumi, Y., and Yoshimori, T. (2000). LC3, a mammalian homologue of yeast Apg8p, is localized in autophagosome membranes after processing. EMBO J. *19*, 5720–5728.

Kamada, Y., Funakoshi, T., Shintani, T., Nagano, K., Ohsumi, M., and Ohsumi, Y. (2000). Tor-mediated induction of autophagy via an Apg1 protein kinase complex. J. Cell Biol. *150*, 1507–1513.

Kihara, A., Noda, T., Ishihara, N., and Ohsumi, Y. (2001). Two distinct Vps34 phosphatidylinositol 3-kinase complexes function in autophagy and carboxypeptidase Y sorting in *Saccharomyces cerevisiae*. J. Cell Biol. *152*, 519–530.

Kirisako, T., Baba, M., Ishihara, N., Miyazawa, K., Ohsumi, M., Yoshimori, T., Noda, T., and Ohsumi, Y. (1999). Formation process of autophagosome is traced with Apg8/Aut7p in yeast. J. Cell Biol. *147*, 435–446.

Kolodkin, A.L., and Tessier-Lavigne, M. (2011). Mechanisms and molecules of neuronal wiring: a primer. Cold Spring Harb. Perspect. Biol. *3*, http://dx.doi.org/10.1101/cshperspect.a001727.

Komatsu, M., Wang, Q.J., Holstein, G.R., Friedrich, V.L., Jr., Iwata, J., Kominami, E., Chait, B.T., Tanaka, K., and Yue, Z. (2007). Essential role for autophagy protein Atg7 in the maintenance of axonal homeostasis and the prevention of axonal degeneration. Proc. Natl. Acad. Sci. USA *104*, 14489–14494.

Lai, T., and Garriga, G. (2004). The conserved kinase UNC-51 acts with VAB-8 and UNC-14 to regulate axon outgrowth in *C. elegans*. Development *131*, 5991–6000.

Lamark, T., Kirkin, V., Dikic, I., and Johansen, T. (2009). NBR1 and p62 as cargo receptors for selective autophagy of ubiquitinated targets. Cell Cycle *8*, 1986–1990.

Lang, T., Schaeffeler, E., Bernreuther, D., Bredschneider, M., Wolf, D.H., and Thumm, M. (1998). Aut2p and Aut7p, two novel microtubule-associated proteins are essential for delivery of autophagic vesicles to the vacuole. EMBO J. *17*, 3597–3607.

Lang, T., Reiche, S., Straub, M., Bredschneider, M., and Thumm, M. (2000). Autophagy and the cvt pathway both depend on AUT9. J. Bacteriol. *182*, 2125–2133.

Lee, J.A. (2012). Neuronal autophagy: a housekeeper or a fighter in neuronal cell survival? Exp. Neurobiol. *21*, 1–8.

Lee, K.M., Hwang, S.K., and Lee, J.A. (2013). Neuronal autophagy and neurodevelopmental disorders. Exp. Neurobiol. *22*, 133–142.

Lin, L., Yang, P., Huang, X., Zhang, H., Lu, Q., and Zhang, H. (2013). The scaffold protein EPG-7 links cargo-receptor complexes with the autophagic assembly machinery. J. Cell Biol. *201*, 113–129.

Lu, Q., Yang, P., Huang, X., Hu, W., Guo, B., Wu, F., Lin, L., Kovacs, A.L., Yu, L., and Zhang, H. (2011). The WD40 repeat PtdIns(3)P-binding protein EPG-6 regulates progression of omegasomes to autophagosomes. Dev. Cell *21*, 343–357.

Maday, S., and Holzbaur, E.L. (2014). Autophagosome biogenesis in primary neurons follows an ordered and spatially regulated pathway. Dev. Cell *30*, 71–85.

Maday, S., Wallace, K.E., and Holzbaur, E.L. (2012). Autophagosomes initiate distally and mature during transport toward the cell soma in primary neurons. J. Cell Biol. *196*, 407–417.

Mahoney, T.R., Liu, Q., Itoh, T., Luo, S., Hadwiger, G., Vincent, R., Wang, Z.W., Fukuda, M., and Nonet, M.L. (2006). Regulation of synaptic transmission by RAB-3 and RAB-27 in *Caenorhabditis elegans*. Mol. Biol. Cell *17*, 2617–2625.

Maniar, T.A., Kaplan, M., Wang, G.J., Shen, K., Wei, L., Shaw, J.E., Koushika, S.P., and Bargmann, C.I. (2012). UNC-33 (CRMP) and ankyrin organize microtubules and localize kinesin to polarize axon-dendrite sorting. Nat. Neurosci. *15*, 48–56.

Manil-Segalen, M., Lefebvre, C., Jenzer, C., Trichet, M., Boulogne, C., Satiat-Jeunemaitre, B., and Legouis, R. (2014). The C. elegans LC3 acts downstream of GABARAP to degrade autophagosomes by interacting with the HOPS subunit VPS39. Dev. Cell *28*, 43–55.

Mao, K., Wang, K., Liu, X., and Klionsky, D.J. (2013). The scaffold protein Atg11 recruits fission machinery to drive selective mitochondria degradation by autophagy. Dev. Cell *26*, 9–18.

Marino, G., Madeo, F., and Kroemer, G. (2011). Autophagy for tissue homeostasis and neuroprotection. Curr. Opin. Cell Biol. *23*, 198–206.

Melendez, A., and Levine, B. (2009). Autophagy in *C. elegans*. WormBook, 1–26.

Melendez, A., Talloczy, Z., Seaman, M., Eskelinen, E.L., Hall, D.H., and Levine, B. (2003). Autophagy genes are essential for dauer development and life-span extension in *C. elegans*. Science *301*, 1387–1391.

Mizushima, N., and Klionsky, D.J. (2007). Protein turnover via autophagy: implications for metabolism. Annu. Rev. Nutr. *27*, 19–40.

Mizushima, N., Yoshimori, T., and Levine, B. (2010). Methods in mammalian autophagy research. Cell *140*, 313–326.

Nelson, J.C., Stavoe, A.K., and Colón-Ramos, D.A. (2013). The actin cytoskeleton in presynaptic assembly. Cell Adh. Migr. *7*, 379–387.

Noda, T., Kim, J., Huang, W.P., Baba, M., Tokunaga, C., Ohsumi, Y., and Klionsky, D.J. (2000). Apg9p/Cvt7p is an integral membrane protein required for transport vesicle formation in the Cvt and autophagy pathways. J. Cell Biol. *148*, 465–480.

Obara, K., Sekito, T., and Ohsumi, Y. (2006). Assortment of phosphatidylinositol 3-kinase complexes–Atg14p directs association of complex I to the pre-autophagosomal structure in *Saccharomyces cerevisiae*. Mol. Biol. Cell *17*, 1527–1539.

Ogura, K., Shirakawa, M., Barnes, T.M., Hekimi, S., and Ohshima, Y. (1997). The UNC-14 protein required for axonal elongation and guidance in *Caenorhabditis elegans* interacts with the serine/threonine kinase UNC-51. Genes Dev. *11*, 1801–1811.

Orsi, A., Razi, M., Dooley, H.C., Robinson, D., Weston, A.E., Collinson, L.M., and Tooze, S.A. (2012). Dynamic and transient interactions of Atg9 with autophagosomes, but not membrane integration, are required for autophagy. Mol. Biol. Cell *23*, 1860–1873.

Otsuka, A.J., Jeyaprakash, A., Garcia-Anoveros, J., Tang, L.Z., Fisk, G., Hartshorne, T., Franco, R., and Born, T. (1991). The *C. elegans* unc-104 gene encodes a putative kinesin heavy chain-like protein. Neuron *6*, 113–122.

Patel, N., Thierry-Mieg, D., and Mancillas, J.R. (1993). Cloning by insertional mutagenesis of a cDNA encoding *Caenorhabditis elegans* kinesin heavy chain. Proc. Natl. Acad. Sci. USA *90*, 9181–9185.

Reggiori, F., and Klionsky, D.J. (2013). Autophagic processes in yeast: mechanism, machinery and regulation. Genetics *194*, 341–361.

Reggiori, F., and Tooze, S.A. (2012). Autophagy regulation through Atg9 traffic. J. Cell Biol. *198*, 151–153.

Reggiori, F., Tucker, K.A., Stromhaug, P.E., and Klionsky, D.J. (2004). The Atg1-Atg13 complex regulates Atg9 and Atg23 retrieval transport from the pre-autophagosomal structure. Dev. Cell *6*, 79–90.

Rudolf, R., Khan, M.M., Wild, F., and Hashemolhosseini, S. (2016). The impact of autophagy on peripheral synapses in health and disease. Front. Biosci. *21*, 1474–1487.

Sakamoto, R., Byrd, D.T., Brown, H.M., Hisamoto, N., Matsumoto, K., and Jin, Y. (2005). The *Caenorhabditis elegans* UNC-14 RUN domain protein binds to the kinesin-1 and UNC-16 complex and regulates synaptic vesicle localization. Mol. Biol. Cell *16*, 483–496.

Sato, M., and Sato, K. (2011). Degradation of paternal mitochondria by fertilization-triggered autophagy in *C. elegans* embryos. Science *334*, 1141–1144.

Schindelin, J., Arganda-Carreras, I., Frise, E., Kaynig, V., Longair, M., Pietzsch, T., Preibisch, S., Rueden, C., Saalfeld, S., Schmid, B., et al. (2012). Fiji: an open-source platform for biological-image analysis. Nat. Methods *9*, 676–682.

Shao, Z., Watanabe, S., Christensen, R., Jorgensen, E.M., and Colon-Ramos, D.A. (2013). Synapse location during growth depends on glia location. Cell *154*, 337–350.

Shehata, M., and Inokuchi, K. (2014). Does autophagy work in synaptic plasticity and memory? Rev. Neurosci. *25*, 543–557.

Shen, K., and Cowan, C.W. (2010). Guidance molecules in synapse formation and plasticity. Cold Spring Harb. Perspect. Biol. *2*, a001842.

Shen, W., and Ganetzky, B. (2009). Autophagy promotes synapse development in *Drosophila*. J. Cell Biol. *187*, 71–79.

Shintani, T., Suzuki, K., Kamada, Y., Noda, T., and Ohsumi, Y. (2001). Apg2p functions in autophagosome formation on the perivacuolar structure. J. Biol. Chem. *276*, 30452–30460.

Smith, C.J., Watson, J.D., Spencer, W.C., O'Brien, T., Cha, B., Albeg, A., Treinin, M., and Miller, D.M., 3rd (2010). Time-lapse imaging and cell-specific expression profiling reveal dynamic branching and molecular determinants of a multi-dendritic nociceptor in *C. elegans*. Dev. Biol. *345*, 18–33.

Son, J.H., Shim, J.H., Kim, K.H., Ha, J.Y., and Han, J.Y. (2012). Neuronal autophagy and neurodegenerative diseases. Exp. Mol. Med. *44*, 89–98.

Stanley, R.E., Ragusa, M.J., and Hurley, J.H. (2013). The beginning of the end: how scaffolds nucleate autophagosome biogenesis. Trends Cell Biol. *24*, 73–81.

Stavoe, A.K.H., and Colón-Ramos, D.A. (2012). Netrin instructs synaptic vesicle clustering through Rac GTPase, MIG-10, and the actin cytoskeleton. J. Cell Biol. *197*, 75–88.

Stavoe, A.K., Nelson, J.C., Martinez-Velazquez, L.A., Klein, M., Samuel, A.D., and Colón-Ramos, D.A. (2012). Synaptic vesicle clustering requires a distinct MIG-10/Lamellipodin isoform and ABI-1 downstream from Netrin. Genes Dev. *26*, 2206–2221.

Suzuki, S.W., Yamamoto, H., Oikawa, Y., Kondo-Kakuta, C., Kimura, Y., Hirano, H., and Ohsumi, Y. (2015). Atg13 HORMA domain recruits Atg9 vesicles during autophagosome formation. Proc. Natl. Acad. Sci. USA *112*, 3350–3355.

Tamura, H., Shibata, M., Koike, M., Sasaki, M., and Uchiyama, Y. (2010). Atg9A protein, an autophagy-related membrane protein, is localized in the neurons of mouse brains. J. Histochem. Cytochem. *58*, 443–453.

Tanida, I., Tanida-Miyake, E., Komatsu, M., Ueno, T., and Kominami, E. (2002). Human Apg3p/Aut1p homologue is an authentic E2 enzyme for multiple substrates, GATE-16, GABARAP, and MAP-LC3, and facilitates the conjugation of hApg12p to hApg5p. J. Biol. Chem. *277*, 13739–13744.

Thompson, O., Edgley, M., Strasbourger, P., Flibotte, S., Ewing, B., Adair, R., Au, V., Chaudhry, I., Fernando, L., Hutter, H., et al. (2013). The million mutation project: a new approach to genetics in *Caenorhabditis elegans*. Genome Res. *23*, 1749–1762.

Tian, Y., Li, Z., Hu, W., Ren, H., Tian, E., Zhao, Y., Lu, Q., Huang, X., Yang, P., Li, X., et al. (2010). *C. elegans* screen identifies autophagy genes specific to multicellular organisms. Cell *141*, 1042–1055.

Torres, C.A., and Sulzer, D. (2012). Macroautophagy can press a brake on presynaptic neurotransmission. Autophagy *8*, 1540–1541.

Tsukamoto, S., Kuma, A., Murakami, M., Kishi, C., Yamamoto, A., and Mizushima, N. (2008). Autophagy is essential for preimplantation development of mouse embryos. Science *321*, 117–120.

Wang, C.W., Kim, J., Huang, W.P., Abeliovich, H., Stromhaug, P.E., Dunn, W.A., Jr., and Klionsky, D.J. (2001). Apg2 is a novel protein required for the cytoplasm to vacuole targeting, autophagy, and pexophagy pathways. J. Biol. Chem. *276*, 30442–30451.

Wang, J., Menon, S., Yamasaki, A., Chou, H.T., Walz, T., Jiang, Y., and Ferro-Novick, S. (2013). Ypt1 recruits the Atg1 kinase to the preautophagosomal structure. Proc. Natl. Acad. Sci. USA *110*, 9800–9805.

Wang, T., Martin, S., Papadopulos, A., Harper, C.B., Mavlyutov, T.A., Niranjan, D., Glass, N.R., Cooper-White, J.J., Sibarita, J.B., Choquet, D., et al. (2015). Control of autophagosome axonal retrograde flux by presynaptic activity unveiled using botulinum neurotoxin type a. J. Neurosci. *35*, 6179–6194.

White, J.G., Southgate, E., Thomson, J.N., and Brenner, S. (1986). The structure of the nervous system of the nematode *Caenorhanditis elegans*. Philos. Trans. R. Soc. Lond. *314*, 1–340.

Wong, Y.C., and Holzbaur, E.L. (2015). Autophagosome dynamics in neurodegeneration at a glance. J. Cell Sci. *128*, 1259–1267.

Wu, F., Li, Y., Wang, F., Noda, N.N., and Zhang, H. (2012). Differential function of the two Atg4 homologues in the aggrephagy pathway in *Caenorhabditis elegans*. J. Biol. Chem. *287*, 29457–29467.

Wu, X., Won, H., and Rubinsztein, D.C. (2013a). Autophagy and mammalian development. Biochem. Soc. Trans. *41*, 1489–1494.

Wu, Y.E., Huo, L., Maeder, C.I., Feng, W., and Shen, K. (2013b). The balance between capture and dissociation of presynaptic proteins controls the spatial distribution of synapses. Neuron *78*, 994–1011.

Wu, Y., Cheng, S., Zhao, H., Zou, W., Yoshina, S., Mitani, S., Zhang, H., and Wang, X. (2014). PI3P phosphatase activity is required for autophagosome maturation and autolysosome formation. EMBO Rep. *15*, 973–981.

Wu, F., Watanabe, Y., Guo, X.Y., Qi, X., Wang, P., Zhao, H.Y., Wang, Z., Fujioka, Y., Zhang, H., Ren, J.Q., et al. (2015). Structural basis of the differential function of the two *C. elegans* Atg8 homologs, LGG-1 and LGG-2, in autophagy. Mol. Cell *60*, 914–929.

Xie, Y., Kang, R., Sun, X., Zhong, M., Huang, J., Klionsky, D.J., and Tang, D. (2015). Posttranslational modification of autophagy-related proteins in macroautophagy. Autophagy *11*, 28–45.

Xilouri, M., and Stefanis, L. (2010). Autophagy in the central nervous system: implications for neurodegenerative disorders. CNS Neurol. Disord. Drug Targets *9*, 701–719.

Yamamoto, A., and Yue, Z. (2014). Autophagy and its normal and pathogenic states in the brain. Annu. Rev. Neurosci. *37*, 55–78.

Yamamoto, H., Kakuta, S., Watanabe, T.M., Kitamura, A., Sekito, T., Kondo-Kakuta, C., Ichikawa, R., Kinjo, M., and Ohsumi, Y. (2012). Atg9 vesicles are an important membrane source during early steps of autophagosome formation. J. Cell Biol. *198*, 219–233.

Yang, P., and Zhang, H. (2011). The coiled-coil domain protein EPG-8 plays an essential role in the autophagy pathway in *C. elegans*. Autophagy *7*, 159–165.

Yang, H.Y., Mains, P.E., and McNally, F.J. (2005). Kinesin-1 mediates translocation of the meiotic spindle to the oocyte cortex through KCA-1, a novel cargo adapter. J. Cell Biol. *169*, 447–457.

Yang, Y., Coleman, M., Zhang, L., Zheng, X., and Yue, Z. (2013). Autophagy in axonal and dendritic degeneration. Trends Neurosci. *36*, 418–428.

Yochem, J., and Herman, R.K. (2003). Investigating *C. elegans* development through mosaic analysis. Development *130*, 4761–4768.

Yorimitsu, T., and Klionsky, D.J. (2005). Atg11 links cargo to the vesicle-forming machinery in the cytoplasm to vacuole targeting pathway. Mol. Biol. Cell *16*, 1593–1605.

Young, A.R., Chan, E.Y., Hu, X.W., Kochl, R., Crawshaw, S.G., High, S., Hailey, D.W., Lippincott-Schwartz, J., and Tooze, S.A. (2006). Starvation and ULK1-dependent cycling of mammalian Atg9 between the TGN and endosomes. J. Cell Sci. *119*, 3888–3900.

Yu, W.H., Kumar, A., Peterhoff, C., Shapiro Kulnane, L., Uchiyama, Y., Lamb, B.T., Cuervo, A.M., and Nixon, R.A. (2004). Autophagic vacuoles are enriched in amyloid precursor protein-secretase activities: implications for beta-amyloid peptide over-production and localization in Alzheimer's disease. Int. J. Biochem. Cell Biol. *36*, 2531–2540.

Yue, Z. (2007). Regulation of neuronal autophagy in axon: implication of autophagy in axonal function and dysfunction/degeneration. Autophagy *3*, 139–141.

Yue, Z., Friedman, L., Komatsu, M., and Tanaka, K. (2009). The cellular pathways of neuronal autophagy and their implication in neurodegenerative diseases. Biochim. Biophys. Acta *1793*, 1496–1507.

Zaffagnini, G., and Martens, S. (2016). Mechanisms of selective autophagy. J. Mol. Biol. *428*, 1714–1724.

Zhang, H., and Baehrecke, E.H. (2015). Eaten alive: novel insights into autophagy from multicellular model systems. Trends Cell Biol. *25*, 376–387.

Zhang, Y., Yan, L., Zhou, Z., Yang, P., Tian, E., Zhang, K., Zhao, Y., Li, Z., Song, B., Han, J., et al. (2009). SEPA-1 mediates the specific recognition and degradation of P granule components by autophagy in *C. elegans*. Cell *136*, 308–321.

Zhang, H., Wu, F., Wang, X., Du, H., Wang, X., and Zhang, H. (2013). The two C. elegans ATG-16 homologs have partially redundant functions in the basal autophagy pathway. Autophagy *9*, 1965–1974.

Zhang, H., Chang, J.T., Guo, B., Hansen, M., Jia, K., Kovacs, A.L., Kumsta, C., Lapierre, L.R., Legouis, R., Lin, L., et al. (2015). Guidelines for monitoring autophagy in *Caenorhabditis elegans*. Autophagy *11*, 9–27.

Zhao, H., Zhao, Y.G., Wang, X., Xu, L., Miao, L., Feng, D., Chen, Q., Kovacs, A.L., Fan, D., and Zhang, H. (2013). Mice deficient in Epg5 exhibit selective neuronal vulnerability to degeneration. J. Cell Biol. *200*, 731–741.